Monthly Notices
of the
ROYAL ASTRONOMICAL SOCIETY

Mon. Not. R. Astron. Soc. **405,** 1253–1270 (2010) doi:10.1111/j.1365-2966.2010.16528.x

Are debris discs self-stirred?

G. M. Kennedy⋆ and M. C. Wyatt

Institute of Astronomy, University of Cambridge, Madingley Road, Cambridge CB3 0HA

Accepted 2010 February 15. Received 2010 February 2; in original form 2009 November 5

ABSTRACT

This paper aims to consider the evidence that debris discs are self-stirred by the formation of Pluto-size objects. A semi-analytical model for the dust produced during self-stirring is developed and applied to the statistics for A-stars. We show that there is no significant statistical difference between fractional excesses of A stars $\lesssim$50 Myr old, and therefore focus on reproducing the broad trends, the 'rise and fall' of the fraction of stars with excesses that the pre-stirred model of Wyatt et al. does not predict. Using a population model, we find that the statistics and trends can be reproduced with a self-stirring model of planetesimal belts with radius distribution $N(r) \propto r^{-0.8}$ between 15–120 au, with width $\mathrm{d}r = r/2$. Discs must have this 15 au minimum radius in order to show a peak in disc fraction, rather than a monotonic decline. However, the marginal significance of the peak in the observations means that models with smaller minimum radii also formally fit the data. Populations of extended discs with fixed inner and/or outer radii fail to fit the statistics, due mainly to the slow 70 μm evolution as stirring moves further out in the disc. This conclusion, that debris discs are narrow belts rather than extended discs, is independent of the significance of 24 μm trends for young A-stars. Although the rise and fall is naturally explained by self-stirring, we show that the statistics can also be reproduced with a model in which discs are stirred by secular perturbations from a nearby eccentric planet. Detailed imaging, which can reveal warps, sharp edges and offsets in individual systems, is the best way to characterize the stirring mechanism. From a more detailed look at β Pictoris Moving Group and TW Hydrae Association A-stars, we find that the disc around β Pictoris is likely the result of secular stirring by the proposed planet at $\sim$10 au; the structure of the HR 4796A disc also points to sculpting by a planet. The two other stars with discs, HR 7012 and η Tel, possess transient hot dust, though the outer η Tel disc is consistent with a self-stirred origin. We suggest that planet formation provides a natural explanation for the belt-like nature of debris discs, with inner regions cleared by planets that may also stir the disc, and the outer edges set by where planetesimals can form.

Key words: circumstellar matter – planetary systems: formation – planetary systems: proto-planetary discs.

1 INTRODUCTION

Debris discs are the discs of dust found around nearby main-sequence stars through their thermal emission (for a recent review see Wyatt 2008). The dust itself is short-lived compared to the lifetime of the star, so is believed to be continually replenished through collisions between km-sized planetesimals (Wyatt & Dent 2002; Quillen, Morbidelli & Moore 2007), much in the same way that the dust in the zodiacal cloud is replenished through collisions in the asteroid belt and Kuiper belt (Dermott et al. 2001; Moro-Martín & Malhotra 2003). While there remain difficulties in growing dust from its initially sub-μm size into >km-sized planetesimals (Blum & Wurm 2008), the widely invoked coagulation and core accretion models for planet formation rely on relative velocities in the protoplanetary disc being low enough that collisions result in net accretion, rather than destruction. As it seems that the opposite is the case in debris discs, these discs must have been stirred at some point so that collisions occur at $\gtrsim$1–10 m s^{-1}, which typically corresponds to eccentricities and inclinations for the disc material of $e \gtrsim 10^{-3}$ to 10^{-2} (e.g. Kenyon & Bromley 2008).

To explain debris discs, it is not normally necessary to understand how (or when) they were stirred. It is sufficient to invoke a 'pre-stirred' debris disc – one that was stirred when the star was born. For example, it is possible to explain the statistics of dust found around A-stars of ages >10 Myr by assuming that all stars are

⋆E-mail: gkennedy@ast.cam.ac.uk

born with a pre-stirred planetesimal belt that evolves due to steady-state collisional erosion (Wyatt et al. 2007b). The diversity seen at different ages then reflects their different initial masses and radii. A similar conclusion was reached for debris discs around sun-like stars (Löhne, Krivov & Rodmann 2008).

However, recent results on the presence of debris discs around young A-stars are challenging this view by showing that the fractional excess at 24 μm from hot dust increases from 3 Myr (the time at which most protoplanetary discs have dissipated) to a peak at ∼10–30 Myr, followed by a slow decline as expected by steady-state evolution (Hernández et al. 2006; Currie et al. 2008a; Currie, Plavchan & Kenyon 2008b). This peak has been interpreted as evidence for self-stirring, where debris are created when the largest objects become massive enough to stir planetesimals to fragmentation velocities.[1]

Self-stirring models follow the evolution of an extended planetesimal belt from the protoplanetary disc stage, allowing both the size distribution and the velocity distribution to evolve in a self-consistent manner. These models find that the stirring of the planetesimal belts occurs when planets reach Pluto-size, which depends strongly on their distance from the star, as well as on the mass surface density of solid material there: $t_{\rm Pluto} \propto P/\Sigma$, where P is the orbital period and Σ is the surface density of planetesimals (e.g. Lissauer 1987). For a typical disc model $\Sigma = \Sigma_0\, r^{-1.5}$, so $t_{\rm Pluto}$ depends strongly on radius r:

$$t_{\rm Pluto} \propto r^3/(\Sigma_0\sqrt{M_\star})\,. \quad (1)$$

Thus, compared to pre-stirred discs, self-stirring means that farther disc regions are stirred at later times because it takes longer for Pluto-size objects to form there. This evolution means that individual discs can show a peak in emission at ∼10–30 Myr, set by the time to form Pluto-size objects at the inner disc edge (Hernández et al. 2006; Currie et al. 2008a; Kenyon & Bromley 2008; Wyatt 2008). That is, the observed evolution occurs if debris discs tend to have ∼10 au inner holes. The overall dust content at <10 Myr is low because such times are needed for Plutos to form at the inner edge of the disc. This lack of dust implies that accretion with minimal fragmentation is ongoing in young (<10 Myr) debris discs and the outer regions of older debris discs.

Though the Kenyon & Bromley (2008) self-stirring models are qualitatively consistent with the ∼10–30 Myr peak in fractional excesses, there has been no quantitative test of whether these models can reproduce the observed A-star statistics, or how the observations constrain disc parameters. In this paper, our aim is to address this issue using the Wyatt et al. (2007a) debris disc evolution model, modified to include self-stirring (as outlined in Wyatt 2008).

In particular, there are several issues to address. Because the peak in excesses occurs when Plutos form at the inner disc edge, the timing of this peak is highly dependent on the radius of the cleared region and on mass surface density (equation 1). Yet we know that protoplanetary discs have a range of masses and surface densities (e.g. Natta, Grinin & Mannings 2000; Andrews & Williams 2005, 2007), and it seems unlikely that the inner clearing would be at the same radius for all discs. Therefore, we wish to find whether self-stirring models can reproduce the A-star statistics, and if so, whether they put a strong constraint on disc inner radii as equation (1) suggests.

[1]Self-stirring is also called delayed stirring in the literature, but following Wyatt (2008) we consider that what we are calling self-stirring is a subset of possible delayed-stirring models.

Another issue is the extent of debris discs. Kalas et al. (2006) note that discs resolved in scattered light appear to be either relatively narrow belts 20–30 au wide, or extended discs wider than 50 au (however, a disc that appears extended may result from blowout of small grains created in a relatively narrow planetesimal belt). In fitting the statistics for ($\gtrsim$10 Myr) A-stars, Wyatt et al. (2007b) considered discs to be the former; belts centred at radial distance r with an assumed width of $\mathrm{d}r = r/2$. However, self-stirring allows the interesting possibility that discs similar in extent to observed protoplanetary discs – from near the star to many hundreds of astronomical units – may evolve to look like narrow belts because only regions of recent Pluto formation may be luminous enough to be detected. Therefore, we also wish to evaluate whether debris discs tend to be 'narrow belts' or 'extended discs' (we use these terms consistently throughout to refer to these types of discs).

A final issue is whether debris discs could be stirred by something other than the formation of Pluto-sized objects. Though self-stirring has been the only proposed mechanism, secular perturbations from planets (another subset of delayed stirring) seems to be an equally viable way to stir debris discs (Mustill & Wyatt 2009). This hypothesis is partly motivated by stars with debris discs known or predicted to harbour planets, such as Fomalhaut and β Pic (Mouillet et al. 1997; Quillen 2006; Kalas et al. 2008; Lagrange et al. 2009b). The question is therefore whether we can identify the more important stirring mechanism, both at a population level and for individual objects.

The layout of this paper is as follows. In Section 2, we outline the Wyatt et al. (2007a,b) model, and the modifications made to include self-stirring. We empirically fit some model parameters to reproduce the self-stirring models of Kenyon & Bromley (2008) in Section 3. As self-stirring results in not only excess evolution, but also spatial evolution as Plutos form farther from the central star, we show how disc surface density profiles evolve and vary with model parameters. In Section 4, a population model is compared with the statistics for A-stars. We briefly consider a planet-stirred population model, take a more detailed look at resolved β Pictoris Moving Group and TW Hydrae A-stars in the context of delayed stirring, and discuss other influences on debris disc structure in Section 5. We summarize our main conclusions in Section 6.

2 ANALYTICAL SELF-STIRRING MODEL

This section describes the analytical model. It is an extension of the model described in Wyatt et al. (2007a,b) to include delayed stirring by splitting discs into a series of concentric annuli. The implementation uses the equations in section 2 of Wyatt et al. (2007a,b) and sums over 100 logarithmically spaced annuli to create a disc with radial extent. The self-stirring prescription is semi-empirical, based on the more detailed models of Kenyon & Bromley (2008) (see section 3.1). Here, we briefly summarize the model and refer the reader to section 2 of Wyatt et al. (2007a,b) for details omitted here.

We use a minimum mass solar nebula (MMSN; Weidenschilling 1977) surface density profile to specify the disc mass

$$\Sigma = \eta M_\star\, \Sigma_0\, r^{-\delta}\,, \quad (2)$$

where η is a scaling parameter reflecting a range of disc masses, $M_\star$ is in solar units, radial distance r is in astronomical units and the surface density at 1 au is $\Sigma_0 = 30$ g cm^{-2} ($1.1\,M_\oplus/\mathrm{au}^2$ in our units). The power-law index δ is typically 1–1.5; we use 1.5 as our canonical value. This surface density provides roughly the amount of solid material contained in the outer Solar system. The

surface density scales linearly with stellar mass, consistent with mm observations of protoplanetary discs. However, the range of stellar masses in our model is much smaller than the expected range of η, so the factor $M_\star$ is relatively unimportant (Natta et al. 2000; Andrews & Williams 2005). For extended discs the inner and outer radii are independent and specified by $r_{\rm in}$ and $r_{\rm out}$. Narrow belts are specified by their radii $r_{\rm mid}$ and width dr (so for belts $r_{\rm in,out} = r_{\rm mid} \pm {\rm d}r/2$).

Where Wyatt et al. (2007b) considered a range of total masses $M_{\rm tot}$, we consider a lognormal distribution about $\eta_{\rm mid}$.[2] There is as yet no evidence of a positive correlation between disc mass and radius (which might argue for the distribution of η to be narrower than that for $M_{\rm tot}$), and thus we use the 1σ width of 1.14 dex observed for disc masses in Taurus (Andrews & Williams 2005).

The planetesimal disc is assumed to be in collisional equilibrium with a size distribution in each annulus defined by $N(D) = KD^{2-3q}$, where K is a constant, $q = 11/6$ for an infinite collisional cascade (Dohnanyi 1969) and D is planetesimal diameter. That distribution is assumed to hold from the largest planetesimal in the disc, of diameter $D_{\rm c}$ (in km), down to the size below which particles are blown out by radiation pressure as soon as they are created, $D_{\rm bl}$ (in μm). If q is in the range 5/3 to 2, then most of the mass is in the largest planetesimals while the cross-sectional area $\sigma_{\rm tot}$ is dominated by the smallest particles:

$$\sigma_{\rm tot} = 3.5 \times 10^{-17} K (3q-5)^{-1} \left(10^{-9} D_{\rm bl}\right)^{5-3q} \quad (3)$$

in au^2.

We assume that particles act like blackbodies, so the fractional luminosity of grains $f = L_{\rm IR}/L_\star = \sigma_{\rm tot}/4\pi r^2$ for the annulus at r. The grain blowout size is

$$D_{\rm bl} = 0.8\,(L_\star/M_\star)\,(2700/\rho)\,, \quad (4)$$

where $D_{\rm bl}$ is in μm, $L_\star$ and $M_\star$ are in Solar units, and density ρ is in kg m^{-3}. The dust temperature can be worked out from

$$T = 278.3\, L_\star^{0.25} r^{-0.5}\,. \quad (5)$$

We also assume that the central star acts like a blackbody.

Because we use a fixed size distribution with $q = 11/6$ in our model, the long-term evolution of the disc is determined by the removal of mass from the top end of the cascade. Planetesimals have a disruption threshold $Q_{\rm D}^\star$ and eccentricity e. The collisional lifetime of the largest planetesimals of size $D_{\rm c}$ at a radius r in an MMSN disc is

$$t_{\rm c} = 2.2 \times 10^{-10} r^{23/6}\, D_{\rm c}\, {Q_{\rm D}^\star}^{5/6}\, e^{-5/3}\, M_\star^{-7/3}\, \Sigma_0^{-1}\, \eta^{-1} \quad (6)$$

in Myr, obtained by substituting $\Sigma = M_{\rm tot}/2\pi r{\rm d}r$ into Wyatt et al. (2007b) equation (9). We have simplified the relation here by assuming that $X_{\rm c} = D_{\rm cc}/D_{\rm c} \ll 1$, where $D_{\rm cc}$ is the smallest planetesimal that has enough energy to catastrophically destroy a planetesimal of size $D_{\rm c}$. This condition applies for the $e \gtrsim 0.01$ eccentricities found for self-stirring models (Wyatt et al. 2007a).

Assuming that collisions are the only process affecting the evolution of the surface density, then

$$\Sigma(r,t) = \begin{cases} \Sigma(r,0) & t < t_{\rm stir} \\ \Sigma(r,0)/[1 + (t - t_{\rm stir}(r))\,/t_{\rm c}(r,0)] & t > t_{\rm stir}, \end{cases} \quad (7)$$

[2]Previously, each disc was assigned a total mass distributed about $M_{\rm mid}$ independent of disc location. This led to typical discs at $r = 120$ au having about six times lower Σ_0 than discs at 3 au (for $\delta = 3/2$). However, this difference is smaller than the dispersion in surface density and disc mass so is not particularly important.

where $\Sigma(0)$ is the initial surface density profile, $t_{\rm stir}$ is the delay until stirring (assumed to be 0 in Wyatt et al. 2007b) and $t_{\rm c}(r,0)$ is the collisional lifetime at r at that initial epoch. Where $t < t_{\rm stir}$, the initial surface density profile applies.

Because more massive discs process their mass faster ($t_{\rm c} \propto 1/\eta$), the surface density at late times ($t \gg t_{\rm c}$ and $t > t_{\rm stir}$) at a given radius is independent of initial surface density. Written in terms of the surface density of cross-sectional area in the disc (or simply 'surface density' because $\tau_{\rm eff} \propto \Sigma$, $\tau_{\rm eff} = \sigma_{\rm tot}/2\pi r{\rm d}r = 2fr/{\rm d}r$),

$$\tau_{\rm eff,max} = 1.2 \times 10^{-9}\, r^{7/3}\, D_{\rm c}^{0.5}\, {Q_{\rm D}^\star}^{5/6} \times e^{-5/3}\, M_\star^{-5/6}\, L_\star^{-0.5}\, (t - t_{\rm stir})^{-1}\,. \quad (8)$$

This prescription means that for a disc of known size at any given age, there is a maximum IR luminosity, $f_{\rm max}$, that can remain due to collisional processing. While $f_{\rm max}$ can be applied to unresolved stars based on the 24–70 μm colour and some assumption about disc extent (Wyatt et al. 2007a), $\tau_{\rm eff,max}$ necessarily requires resolved observations for comparison. We return to the application of $\tau_{\rm eff,max}$ to self-stirred discs in Section 3.3.

The final component of the model is the implementation of self-stirring, where successive annuli can be stirred at later times with increasing r (such as equation 1). Other mechanisms for delayed-stirring, such as secular perturbations from an eccentric planet (e.g. Mustill & Wyatt 2009), can be implemented with different $t_{\rm stir}$ (see Section 5.1). The introduction of self-stirring also requires us to specify the level of disc emission before a disc is stirred. We assume that the emission is proportional to the surface density, but reduced by a factor $x_{\rm delay}$ with respect to that expected from equation (3) because the collisional cascade has not yet begun. We estimate $x_{\rm delay}$ through comparison with the Kenyon & Bromley (2008) models below.

3 DEBRIS DISC EVOLUTION FOR INDIVIDUAL STARS

In this section, we consider model evolution for individual discs, first making comparisons with the Kenyon & Bromley (2008) models, and then illustrating the surface density evolution. We then consider the implications for transience in the context of the Wyatt et al. (2007a) model and the effects of disc extent on excess evolution.

3.1 Comparison with Kenyon & Bromley models

We compare our model with the Kenyon & Bromley simulations of planet formation and debris disc evolution around A-stars to derive an empirical self-stirring time and $x_{\rm delay}$ that reproduces their excess evolution. Though Kenyon & Bromley (2008) derive relations for the time to reach the peak excess (their equation 55), and the radial time dependence for forming 1000 km objects (their equation 41), they do not derive a relation for the peak excess at different radial locations. Because our aim is to reproduce their excess evolution, we use the following empirical relation:

$$t_{\rm stir} = 4 \times 10^{-4}\, r^3\, \eta^{-1/2}\, M_\star^{-3/2} \quad (9)$$

in Myr. We first derived the numerical pre-factor and the exponent of η in this relation with a χ^2 minimization procedure over models with $1.5 < M_\star < 3$ and $1/3 < \eta < 3$ at 24 and 70 μm. We fix the radial and stellar mass dependence because these are set by the orbital period and our assumption of $\Sigma \propto M_\star$. However, this formal method ignores some important model differences, in particular the continued stirring that appears to cause the Kenyon & Bromley (2008) models to decay faster at 70 μm (discussed below).

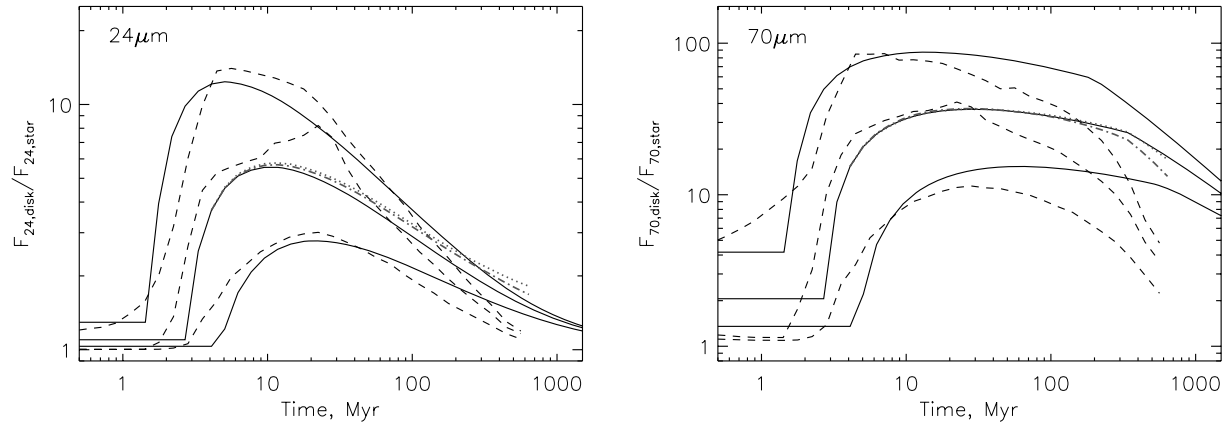

Figure 1. Evolution of 24 μm (left-hand panel) and 70 μm (right-hand panel) excesses for $\eta = 1/3$, 1, and 3 for a disc from 30 to 150 au from our model (solid lines) compared to models from Kenyon & Bromley (2008) (dashed lines), for an A2 (2.5 $M_\odot$) star. The main difference between the models at 70 μm is caused by continued accretion and subsequent stirring in the Kenyon & Bromley (2008) models (see text). Also shown is the effect of the increasing main-sequence luminosity on an $\eta = 1$ disc with $D_{bl} = 1$ μm (grey dotted line) and then also allowing D_{bl} to vary (grey dot–dashed line). The overall effect of stellar evolution due to changing D_{bl} and hotter grains (i.e. dot–dashed line) is a small increase in 24 μm excesses and a similar decrease in 70 μm excesses.

We therefore arrive at equation (9) by focusing on the 24 μm peak excesses. This different emphasis changes the values obtained in the formal fit at 24 μm by ∼10–20 per cent.[3]

Though the dependence on η in equation (9) is weaker than implied by equation (1) ($-1/2$ versus -1), the two should not necessarily agree. Kenyon & Bromley (2008) find that the time to peak dust production is $\propto \eta^{-1} M_\star^{-1.5}$ (as predicted by equation 1), but that the time to peak luminosity is $\propto \eta^{-2/3} M_\star^{-1}$ and takes much longer (their equations 48 and 55). In comparing these proportionalities, it is important to remember that the peak dust production and peak luminosity are linked, but not directly. The observed luminosity depends on the history of the dust production rate and the rate at which small grains are being removed by radiation forces. Further, our empirical relation sets the evolution at specific r, rather than describing the global evolution of specific disc properties. Though equation (9) is derived largely from the 24 μm evolution, we reproduce the f evolution, from which the Kenyon & Bromley peak luminosity is derived equally well. Our scaling of t_{stir} with η is probably weaker than their $-2/3$ because we set the *onset* of stirring, not the peak excess and higher mass discs reach their peak excess more rapidly once stirring starts (Fig. 1). We refer to the radial location where stirring has just begun (i.e. where $t = t_{stir}$) as r_{stir}.

Fig. 1 shows a comparison of the Kenyon & Bromley model for an A2 (2.5 $M_\odot$) star with an equivalent one from our model. The 24 μm excess increases to a peak around 10 Myr, and then declines (see Hernández et al. 2006; Currie et al. 2008a; Kenyon & Bromley 2008; Wyatt 2008, for comparison with observations). In this example, the disc extends from 30–150 au, and has $\eta = 1/3$, 1 and 3. We set the level of disc emission before stirring to $x_{delay} = 0.01$, which gives a reasonable match to the excesses prior to the formation of Pluto size objects. We take other model parameters from the best-fitting model of Wyatt et al. (2007b); $e = 0.05$, $D_c = 60$ km and $Q_D^\star = 150$ J kg^{-1}. Though the largest objects in the disc are roughly Pluto size when the collisional cascade begins, Kenyon & Bromley find that objects larger than ∼1–10 km continue growing. Thus, the effective maximum planetesimal size D_c for our model is of the order of 10 km because the smallest dust derives from a reservoir of objects of this size. Different choices for D_c, e and $Q_D^\star$ change the rate at which excesses increase after the disc is stirred, though still give peak excesses that agree with the Kenyon & Bromley models within factors of a few.

To achieve the agreement shown in Fig. 1, we must temporarily modify our model to match some Kenyon & Bromley assumptions about dust properties; they set $D_{bl} = 1$ μm and use a 'greybody' emission law $F_\nu \propto B_\nu(T)(1 - \exp(\lambda_0/\lambda))$ with $\lambda_0 = 10$ μm. They use Yi et al. (2001) luminosities, somewhat brighter than the Schmidt-Kaler (1982) luminosities used in our model. Finally, to ensure a good match between models we apply a factor of 2.5 decrease to the Kenyon & Bromley excesses. The need for this factor is unsurprising considering the model differences and could, for example, arise from differences of a few per cent in the average size distribution index q between D_c and D_{bl}. With these differences taken into account, both models produce fairly similar results. The delay in the rise of 24 and 70 μm excesses is similar, as are their magnitudes over the range A0–F2 (∼1.5–3 $M_\odot$) and $\eta = 1/3$–3.

The main difference is the decline in 70 μm excesses at late times. Our model shows a fairly slow decline until after 200–600 Myr, when stirring reaches the outer disc edge and the excess decreases more rapidly because mass is being lost at all radii. The Kenyon & Bromley (2008) models show a faster decay. In their model, the largest objects continue to accrete once they reach Pluto size, thus increasing the rate of decay through removal of mass from the collisional cascade. More important is the increased stirring due to their continued growth and the subsequent higher collision rates (S. Kenyon, Private communication). This importance can be understood from the strong e dependence in equation (6).

Fig. 1 also shows the effect of including stellar evolution in our model (scaled to show relative differences). For fixed D_{bl}, increasing $L_\star$ increases grain temperatures and the 24 μm excess is higher. If D_{bl} is allowed to vary, the disc emission drops slightly due to smaller σ_{tot} as D_{bl} increases and the overall effect is a small increase in 24 μm emission and a similar decrease at 70 μm.

[3]Similar variation is also found depending on how the Kenyon & Bromley models are weighted in the minimization procedure. For example, lower weights for smaller excesses makes the peak excesses fit better, whereas constant weights fit the late time evolution better but underestimates the peak excesses. Allowing x_{delay} to vary results in values in the range of ∼0.01–0.02.

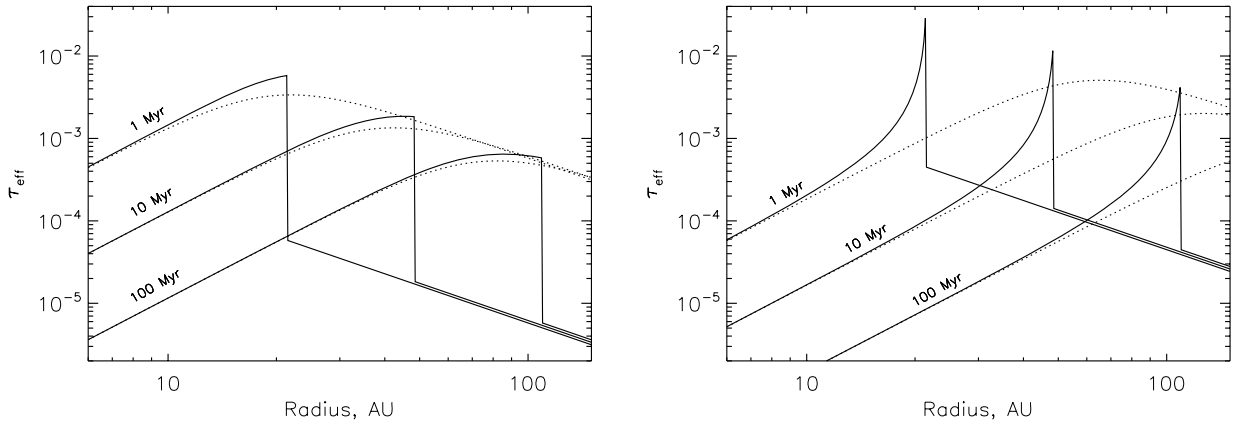

Figure 2. Evolution of $\tau_{\rm eff}$ for self-stirred (solid lines) and pre-stirred (dotted lines) discs at 1, 10 and 100 Myr. In the left-hand panel $t_{\rm c} \gg t_{\rm stir}$, so evolution is 'slow' and similar to the pre-stirred case. In the right-hand panel $t_{\rm c} \ll t_{\rm stir}$ so the evolution at $r_{\rm stir}$ is 'fast' and much more violent as the disc reverts to the equilibrium state. Lines are offset slightly to remove ambiguities. The discs extend from 5–150 au around an A2 star and have parameters: $\eta = 1$, $Q_{\rm D}^{\star} = 150$ J kg^{-1}, $e = 0.05$, $x_{\rm delay} = 0.01$ and $D_{\rm c} = 60$ km (left-hand panel) and $D_{\rm c} = 1$ km (right-hand panel). The peak surface density is larger for the fast self-stirred disc because more mass is concentrated in smaller size objects.

After a few hundred Myr, the Kenyon & Bromley 70 μm excesses also show a break towards faster decay. They attribute this decrease to stellar evolution as the star nears the end of its main-sequence lifetime (of 650 Myr for 2.5 $M_{\odot}$). Higher stellar luminosity increases the importance of Poynting-Robertson (PR) drag relative to collisions and the disc emission drops more rapidly as grains spiral towards the star. However, any mass lost to PR drag is probably due to the assumption of a fixed $D_{\rm bl}$, as these models are of observable discs, which are generally not tenuous enough to suffer PR drag before grains collide (Wyatt 2005). For the A2 star in Fig. 1, $D_{\rm bl}$ should increase from about 10 to 20 μm during the main-sequence lifetime, so fixing $D_{\rm bl} = 1$ μm allows PR drag to remove grains that would have instead been blown out of the system. Also, a disc is unlikely to become PR dominated by realistic increases in stellar luminosity.[4] Our model shows a break at 200 Myr for the $\eta = 3$ (top) line at 70 μm when stirring reaches the outer edge of the disc. Given that PR drag is unlikely to be the cause, the further drop in the Kenyon & Bromley models after ∼200 Myr may in part be for the same reason.

In summary, we have shown that our simplified model is in good agreement with the Kenyon & Bromley (2008) models, with the main remaining discrepancies arising for older stars at 70 μm. The effect of changing main-sequence luminosities is small, and continued accretion by the largest bodies leads to smaller 70 μm excesses after the peak is reached. We retain our prescription for $D_{\rm bl}$, the main cause of the initial differences because it is well established that grains should respond to radiation forces (e.g. Burns, Lamy & Soter 1979). We allow $x_{\rm delay}$ to vary, though it is usually unimportant because most emission comes from stirred regions.

3.2 Evolution of surface brightness

Debris discs around some of the closest stars have been resolved, providing spatial information that cannot be derived from unresolved photometry. In this section, we show disc profiles derived from our model for comparison. With delayed stirring, there are two possible ways for the disc to evolve when stirring begins. These are set by the collisional ($t_{\rm c}$) and stirring ($t_{\rm stir}$) times. These two modes of evolution are shown in Fig. 2, which shows the $\tau_{\rm eff}$ evolution versus radius in an extended disc at several times.

In Fig. 2, we also compare the evolution with a pre-stirred disc – one that is stirred when the star is born at $t = 0$ (dotted lines). In this case, the surface density profiles increase with radius to a broad peak. The slope of the inner region, where mass at all radii is being depleted collisionally, is set by $\tau_{\rm eff,max} \propto r^{7/3}$ (equation 8). Outside the peak, the primordial $\tau_{\rm eff}$ remains because the collisional time is longer than the disc age there (i.e. $\tau_{\rm eff,max} \propto r^{-3/2}$). The location of the peak moves outwards with time ($r \propto t^{6/23}$, equation 6) as more distant regions begin to decay.

The solid curves in Fig. 2 (left-hand panel) show the self-stirred evolution when the collisional time is longer than the stirring time. Compared to the pre-stirred case, the difference is the $x_{\rm delay}$ drop outside $r_{\rm stir}$ where the disc has not been stirred and accretion is ongoing. For this disc, little decay happens at $r_{\rm stir}$ immediately, but begins later when $t > t_{\rm c}$. This evolution is therefore similar to the pre-stirred case, and we term this mode of evolution 'slow' for a self-stirred disc. Compared to a pre-stirred disc, the factor $x_{\rm delay}$ leads to a narrower observed annulus if the disc is too faint to be detected outside $r_{\rm stir}$. For comparison, see fig. 9a of Kenyon & Bromley (2004), which shows a qualitatively similar profile.

In the other limit, when the collisional time is shorter than the stirring time (Fig. 2, right-hand panel), for a given age the disc at $r_{\rm stir}$ has much more mass than it would if it were pre-stirred (the same mass as at $t = 0$). The onset of stirring is therefore violent, with the rapid shedding of mass just inside $r_{\rm stir}$ as the disc reverts to its 'equilibrium' state, that of a pre-stirred disc where the decay is independent of initial mass. This evolution was hinted at by Dominik & Decin (2003), where the excesses of discs with longer delay times decayed faster with time (their Fig. 3). We call this evolution the 'fast' mode. These discs appear transient because the surface density can be significantly above the expected pre-stirred level for their age (see Section 3.3).

However, we consider fast self-stirred discs with very sharp surface density profiles unlikely, because discs with short collisional times will start to decay before Pluto-size objects form. Planetesimal

[4]For fixed $M_{\star}$ and r, the orbit decay time-scale for smallest grains (which are most affected by PR drag) is $t_{\rm PR} \propto D_{\rm bl}/L_{\star}$. However, because $D_{\rm bl}$ increases with $L_{\star}$ (equation 4), the PR time-scale for the smallest grains is constant. The collisional lifetime of the smallest grains increases slowly as $t_{\rm coll} \propto \sqrt{D_{\rm bl}}$. For fixed $\beta = 0.5$, the relative importance of PR drag versus collisions $\eta_0 \equiv t_{\rm PR}/t_{\rm coll} \propto 1/\sqrt{L_{\star}}$, and therefore changes little for the factor ∼few changes in main-sequence $L_{\star}$.

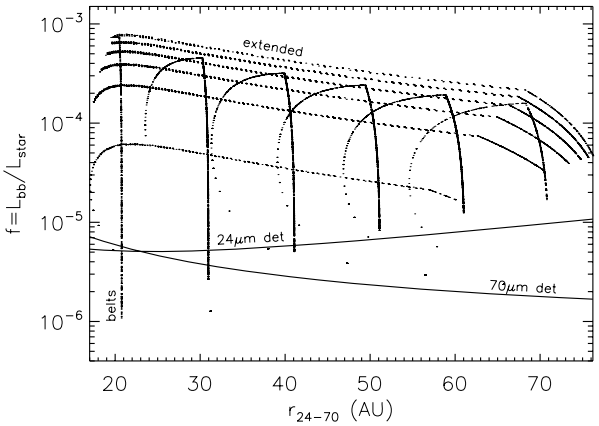

Figure 3. Evolution of narrow belts and extended discs (as labelled) in f versus r_{24-70} space from 1 Myr to 1 Gyr. Disc r_{24-70} increases as stirring moves outwards (so evolution is left to right). Here, f is derived from a blackbody at r_{24-70} (i.e. what detection at 24 and 70 μm would imply). Solid lines show 24 and 70 μm blackbody detection limits from Wyatt et al. (2007b). Extended discs have $r_{\rm in-out} = 15$–120 au and $\eta = 0.05$–1.05. For belts $r_{\rm mid} = 20$, 30, 40, 50, 60 and 70 au, $\mathrm{d}r = r_{\rm mid}/2$ and $\eta = 1$. Belts increase in radius from left to right, and extended discs increase in f with higher η. Other model parameters are as in the left-hand panel of Fig. 2.

eccentricities increase as the largest objects grow, and $t_{\rm c}$ decreases accordingly. Thus, a disc that would stir in the fast mode in our model would in fact begin to decay earlier when $t > t_{\rm c}$ (unless planetesimal eccentricities increase rapidly, in which case the time difference is small).[5] Because the largest objects continue to grow after the disc is stirred, eccentricities continue to increase. After stirring, $t_{\rm c}$ continues to decrease until the disc begins to decay. Thus, we also do not expect discs where the stirring time is significantly shorter than the collision time.

By equating the stirring and collisional time-scales (equations 9 and 6), we can derive the conditions required for the boundary between these regimes of evolution at $r_{\rm stir}$ (assuming $X_{\rm c} \ll 1$). Evolution will be 'slow' at $r_{\rm stir}$ if

$$\mathcal{R} \equiv r_{\rm stir}^{5/6}\, D_{\rm c}\, {Q_{\rm D}^{\star}}^{5/6}\, e^{-5/3}\, M_{\star}^{-5/6}\, \eta^{-1/2} > 2 \times 10^{6}\,. \quad (10)$$

At 50 au on the 10 Myr curves, the discs illustrated in Fig. 2 have $\mathcal{R} = 4 \times 10^6$ (left-hand panel) and 6×10^4 (right-hand panel), two times greater and 33 times smaller than condition (10), respectively. Because the collisional time increases more strongly with distance than the stirring time, inner disc regions are more prone to fast evolution, as are discs with weak or small planetesimals. There is some tendency towards fast evolution for more massive discs, though if the stirring time were simply the Pluto formation time (equation 1), this condition would be independent of surface density. Because discs with $\mathcal{R} \sim 10^6$ are the most physically plausible within our model, we check the distribution of $\mathcal{R}$ when generating population models in Section 4.

The evolution of slow self-stirred discs makes clear predictions for resolved observations of debris discs. While the brightest discs will yield broad surface density profiles, fainter discs only have an annulus of detectable emission because the surface density drops away interior and exterior to where the peak emission occurs. The observed width of the disc depends on how fast the disc is decaying relative to its age; however, we do not expect surface density profiles as sharp as shown in the right-hand panel of Fig. 2 for self-stirred discs. Of course, the disc extent is also set by where planetesimals can form and where they are not affected by external effects such as clearing, accretion or ejection by planets.

For slow self-stirred discs, the peak emission is set by the collisional time (i.e. the peak surface density in the left-hand panel of Fig. 2 is slightly interior to $r_{\rm stir}$ at 100 Myr)

$$r \propto t^{6/23}\,. \quad (11)$$

If the difference between the level of emission at the peak and at $r_{\rm stir}$ is small (as in the left-hand panel of Fig. 2 at 1 Myr), and the disc beyond $r_{\rm stir}$ is too faint to detect, then the outer edge of slow self-stirred discs will still appear to increase with time as $r \propto t^{1/3}$ (equation 9).

3.3 Transience

In the Wyatt et al. (2007a) model, narrow pre-stirred planetesimal belts have a maximum luminosity. This property arises because the decay time depends on the disc mass, and all discs were assumed to be stirred at $t = 0$. With an assumption about their width $\mathrm{d}r$, the value $f_{\rm max}$ can be calculated for unresolved belts with observations in several bands, which gives an estimate of their radii. If the disc luminosity is significantly higher than $f_{\rm max}$, the excess is unlikely to arise from steady-state evolution.

Ideally, comparisons would be made between resolved discs and the predicted maximum surface density $\tau_{\rm eff,max}$. As discussed above, we do not expect self-stirred discs to have $\tau_{\rm eff}$ significantly greater than $\tau_{\rm eff,max}$; those that do may be transient. However, because discs may be secularly stirred in the fast mode (Section 5.1), they can appear transient without being so in the sense meant by Wyatt et al. (2007a). Another issue, whether discs are extended or narrow belts is important because discs that are truly transient may not appear to be if they are assumed to be wider than they actually are. Therefore, if discs are narrow belts then $f_{\rm max}$ is a reasonable indicator of transience.

3.4 Radius evolution

There are considerable differences between the evolution of narrow belts and extended discs. Fig. 3 shows the f versus r_{24-70} evolution for discs extending from 15–120 au for a range of initial surface densities, and a series of narrow belts with the same surface density centred at different $r_{\rm mid}$ between 20 and 70 au (r_{24-70} is the radius inferred from the 24–70 μm colour assuming blackbody grains at a single temperature, equation 5).

For extended discs, r_{24-70} increases as $r_{\rm stir}$ moves outwards. The disc r_{24-70} is located between the inner edge and where the surface density peaks, so moves outwards with time. It is not simply at the peak surface density because the inner disc contribution to the spectral energy distribution (SED) is non-negligible when $\tau_{\rm eff} \propto r^{7/3}$. Thus, for extended discs, the increase in r_{24-70} with time is in fact slower than expected by equation (11). The fractional excess decreases somewhat because the decay of emission interior to $r_{\rm stir}$ is stronger than the increased emission from newly stirred regions.

In contrast, belts show a small change in radius and then decay at near constant radius once stirred to the outer disc edge. The narrower disc extent means that r_{24-70} is nearer the peak excess. When stirring reaches the outer edge, all discs break to a faster decline in f because no new regions can be stirred. Because the peak surface density is still evolving outwards (i.e. these discs are evolving in the slow mode), r_{24-70} continues to increase. When

[5] In Section 5.1, we show that discs that evolve in the fast mode are possible if the stirring mechanism is secular perturbations from an eccentric planet.

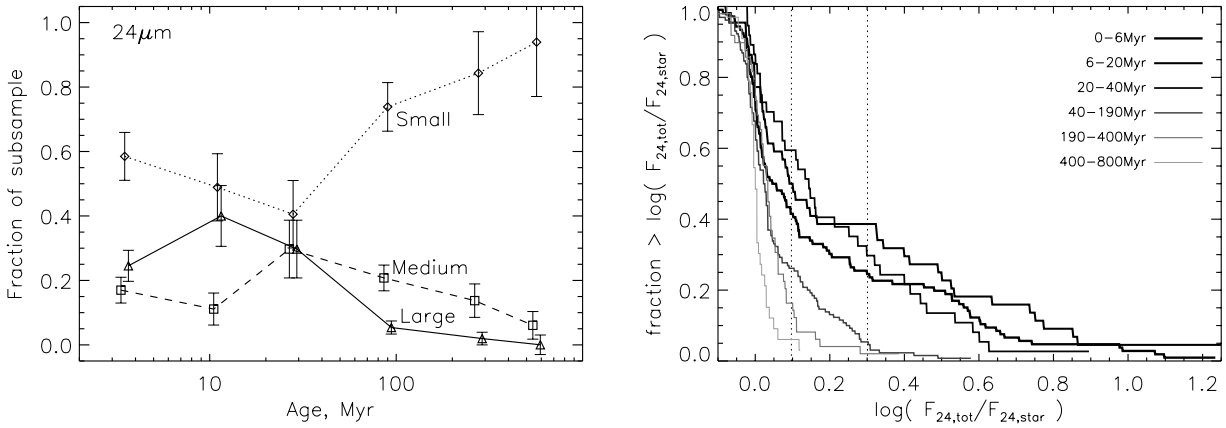

Figure 4. Evolution of A-star 24 μm excesses. The left-hand panel shows stars binned by age and large (triangles), medium (squares) and small (diamonds) excesses (ages offset slightly for clarity). Error bars are $\sqrt{N}$ in each bin and for the oldest large excess bin we assume one disc to calculate the error. Excesses reach an overall peak around 30 Myr. The right-hand panel shows cumulative distributions of 24 μm excesses for the same age bins, from dark to light grey lines. The dotted lines indicate the bin edges for small, medium and large excesses. In the second youngest bin HR4796A and β Pic are beyond the right edge of the plot.

$t \gg t_c$ at the outer edge, f decreases at constant r_{24-70} (because the disc has $\tau_{\rm eff} \propto r^{7/3}$ everywhere and r_{24-70} cannot change). Because the collision time-scales more strongly with radius than stirring ($t_c \propto r^{23/6}$ versus $t_{\rm stir} \propto r^3$), most discs do not reach evolution at constant r_{24-70} until long after the outer disc edge is stirred (and long after the maximum 1 Gyr age shown in Fig. 3). That is, slow evolution is more likely to occur at large radii (equation 10).

For comparison, pre-stirred discs show similar trends to Fig. 3, but f can only decrease because pre-stirred discs start evolving at $t = 0$ everywhere. Thus, pre-stirred discs do not show the initial increase in f seen for the self-stirred evolution. Also, there is no break to a faster decline in f, as occurs when self-stirring reaches the outer disc edge.

4 APPLICATION TO A-STAR STATISTICS

In this section, we apply our model to evolution of 24 and 70 μm excesses around A-stars. We first outline the observations and the limitations of the pre-stirred model. Our aim is to test whether self-stirring can successfully reproduce the rise in 24 μm emission at ∼10–30 Myr (and the 24 and 70 μm statistics at other times), and see what constraints the statistics set on model parameters.

4.1 The A-star sample

The observations are compiled from several sources. Rieke et al. (2005) and Su et al. (2006) observed large unbiased samples of A-stars at 24 and 70 μm with *Spitzer*. While these samples provided the basis for the Wyatt et al. (2007b) study of pre-stirred evolution, they comprise stars mostly older than 10 Myr.

To supplement these data, we collect 24 μm data for B8–A9 stars in the following young clusters/associations: σ Ori (Hernández et al. 2007), OB1a/b (Hernández et al. 2006), λ Ori (Hernández et al. 2009), γ Velorum (Hernández et al. 2008), Upper Sco (Carpenter et al. 2009), β Pic Moving Group (BPMG; Rebull et al. 2008),[6] NGC 2232 (Currie et al. 2008b) and IC 2391 (Siegler et al. 2007). We use the $K_s-[24]$ excess to derive $F_{24,\rm disc}/F_{24,\star}$ for these objects and use spectral types from Kharchenko (2001) where needed. These data make a sample of about 400 A-stars observed at 24 μm with ages between ∼3–800 Myr. All stellar photospheres in these samples are detectable and there are no upper limits (i.e. disc detections are calibration limited). We do not include stars in more distant regions, where observations are sensitivity limited and excess fractions are lower limits.

Because our 24 μm sample includes stars younger than 10 Myr old, it is possible that some are protoplanetary discs. However, consistently shorter disc lifetimes around intermediate mass stars mean that few A-star protoplanetary discs survive beyond a few Myr (Kennedy & Kenyon 2009). Indeed, we exclude only three stars: V346 Ori in OB1a, HD 290543 in OB1b and HD 245185 in λ Ori, which have $K_s - [24] \approx 6.5$–7.5 and strong near IR excesses (Hernández et al. 2006). Less certain is whether the youngest stars in our sample contain dust left over from the protoplanetary disc phase, rather than from that created by fragmentation from self-stirring (e.g. Wyatt 2008).

Fig. 4 (left-hand panel) shows the 24 μm excesses as a function of time binned into 'large' ($F_{24,\rm tot}/F_{24,\star} > 2$), 'medium' ($1.25 < F_{24,\rm tot}/F_{24,\star} < 2$) and 'small' ($F_{24,\rm tot}/F_{24,\star} < 1.25$) excesses. The age bins are 0–6 , 6–20, 20–40, 40–190, 190–400 and 400–800 Myr. There are 106, 45, 37, 130, 51 and 33 stars in these bins, respectively. The primary result at 24 μm is a decline in excesses on a ∼150 Myr time-scale (Rieke et al. 2005).[7] The large and medium excess bins add to give a peak in debris disc fraction at 30 Myr (e.g. Currie et al. 2008b). By separating the excesses into three bins, there is perhaps evidence for an additional trend: the large excesses peak around 10 Myr, and the medium excesses peak around 30 Myr. This behaviour suggests a population of large excess discs that forms around 10 Myr, and then decays relatively rapidly to produce the medium excess population a few tens of Myr later.

Though these features are tantalizing evidence of systematic trends that may be caused by self-stirring, their existence is motivated more by expectations than by statistical significance. In

[6] β Pic is removed from the Rieke et al. (2005) sample. We set the excesses of the Be stars HD 21362 (Rieke sample), HD 67985 (γ Vel) and HIP 78207 (Upper Sco) to $F_{24,\rm tot}/F_{24,\star} = 1$.

[7] This decay is more obvious when viewed on a linear-time plot (e.g. Rieke et al. 2005; Su et al. 2006; Wyatt et al. 2007b) and is only seen in the oldest three bins in Fig. 4.

addition, Carpenter et al. (2009) note that because A-stars take ∼10 Myr to reach the main-sequence, stars of fixed spectral type decrease in luminosity from 1–10 Myr. The decreasing luminosity decreases $D_{\rm bl}$, and can cause at least some of the rise in 24 μm excesses that has been attributed to self-stirring. Using the cumulative distributions shown in Fig. 4 (right-hand panel), we estimate the significance of changes between different age bins with the Kolmogorov-Smirnov (KS) test. According to this test, each pair of cumulative distributions for the three youngest bins (three upper curves) could have all come from the same distribution (max KS probability of difference is 82 per cent). There is at least a 99 per cent chance that all other combinations of distributions are not drawn from the same distribution, with the exception of the fourth age bin when compared to the fifth age bin (78 per cent). That is, there is a robust decay in excesses from early to late times. For the individual clusters collected above, aside from the 50 Myr IC 2391, there is no pair different at more than the 98 per cent level according to the KS test, though NGC 2232 is different from σ Ori, Orion OB1b and γ Vel at 93–98 per cent, and Upper Sco is different from the BPMG at 92 per cent. Therefore, while there are interesting trends at early times, the only formally secure result is that 24 μm excesses decrease after ∼50 Myr.

While there are far fewer observations of A-stars at 70 μm, we use the Su et al. (2006) stars, comprising 153 stars (including 19 observed with *IRAS*, and excluding Be stars HD 21362 and HD 58715 and Herbig Ae/Be star HD 58647). These data include many upper limits, which are largely for stars farther than 100 pc. For the model comparison undertaken here, we use the sample as given by table 4 of Su et al. (2006) (shown in fig. 9 of that paper, or fig. 2 of Wyatt et al. 2007b). As in Su et al. (2006) and Wyatt et al. (2007b), the data are binned into 'large' ($F_{70,\rm tot}/F_{70,\star} > 20$), 'medium' ($5 < F_{70,\rm tot}/F_{70,\star} < 20$) and 'small' ($F_{70,\rm tot}/F_{70,\star} < 5$) excesses. The data are also binned by age: 0–30, 30–190, 190–400 and 400–800 Myr.

The inclusion of upper limits in the 70 μm sample means that the excess fractions are upper limits. As a check, we compare this sample to an unbiased subset of stars closer than 100 pc (and exclude *IRAS* sources, all but 2/19 of which are upper limits). In this subset, only two stars (HD 27962 and HD 142703) with upper limits fall above the small excess bin (with $F_{70,\rm tot}/F_{70,\star} < 5.61$ and <7.63, respectively). The only significant difference between these two samples lies in the youngest age bin, where the <100 pc subset has only one star (of 11) with a small excess, compared to 16 (of 31) for the full sample. This difference arises because the main sample includes many Upper-Sco sources (∼150 pc away) that have upper limits in the small excess bin. However, the paucity of young star-forming regions within 100 pc also results in poor statistics in this bin (with only 11 stars). An alternative approach, setting all stars with upper limits to have small excesses, gives a ∼10 per cent increase in small excesses for the youngest two age bins, and little difference for the older two. For both approaches, there is little change in the excess fractions in all but the youngest age bin (relative to Poisson errors). Based on these comparisons, we conclude that differences in the youngest age bin simply reflect poor statistics due to a lack of very close young stars. The small differences between (sub)samples in the older age bins mean that sample choice does not affect our results. Thus, we use the entire Su et al. (2006) 70 μm sample for comparison with our model.

Fig. 5 shows the evolution of excesses at 70 μm. As with the older age bins at 24 μm, these decay monotonically with time, but with a slower time-scale of $\gtrsim$400 Myr (Su et al. 2006). A KS test shows that the differences between adjacent age bins are not particularly strong (∼90–98 per cent chance of not being from the same distribution), but it is very unlikely that non-adjacent bins could be taken from the same distribution (with probabilities >99.99 per cent). Therefore, the decay from a higher to lower fraction of 70 μm excesses over time is robust.

Finally, we use the Wyatt et al. (2007b) 46 star subsample of stars for which excess emission has been detected at both 24 and 70 μm by *Spitzer* (or 25 and 60 μm by *IRAS*). With the assumption of blackbody grains at a single temperature, this sample provides a set of disc radii (r_{24-70}) for comparison with our model.

4.2 Method

We now explore various population models and their ability to reproduce the A-star statistics. For these models, we select 30 000 stars randomly in the spectral type range B8–A9 with uniform log(age), assuming all stars are born with planetesimal discs. As in Wyatt et al. (2007b), we fix some parameters and allow others to vary. We fix $\rho = 2700$ g cm^{-3}, $q = 11/6$, $I = e$ and do not consider the effects of varying them. These assumptions leave $Q_{\rm D}^{\star}$, $D_{\rm c}$, e, η and the disc radii as parameters.

In addition to comparison of fractional excesses in different age bins, our modelling process also involves comparison of model and observed disc radius distributions using r_{24-70}.

The low significance of the 24 μm trends means that we measure the ability of the self-stirring model to fit A-star statistics at early

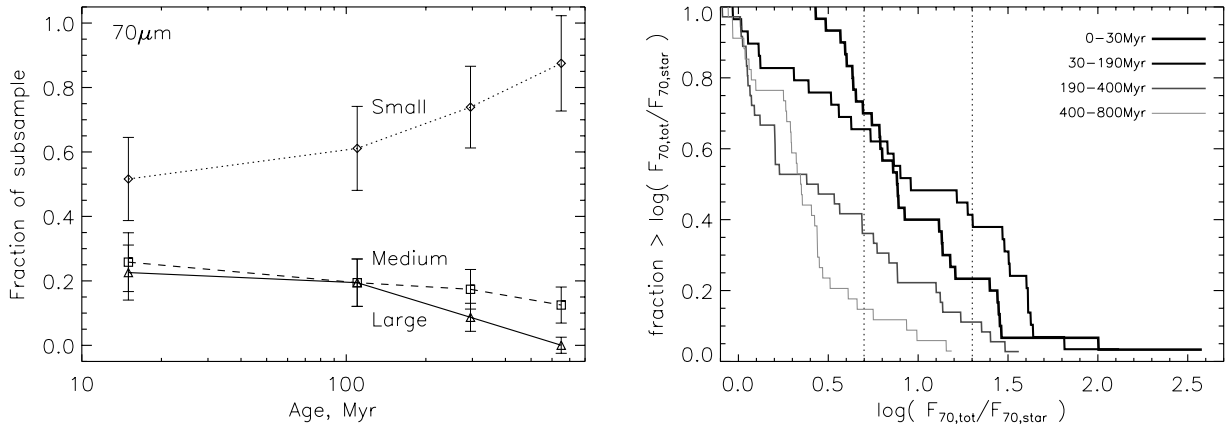

Figure 5. Same as in Fig. 4, but for 70 μm excesses.

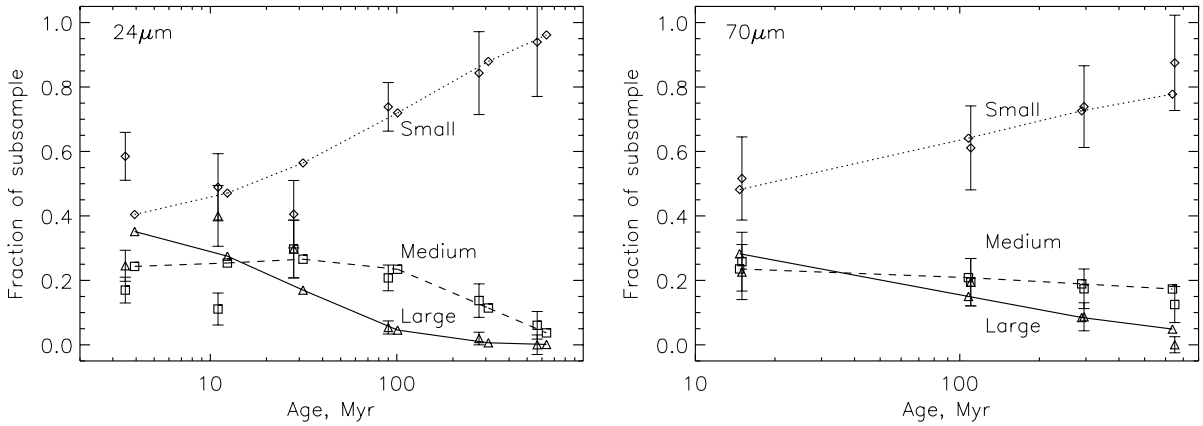

Figure 6. Best-fitting parameters for the Wyatt et al. (2007b) pre-stirred model at 24 and 70 μm (same symbols as Fig. 4, joined by solid, dashed and dotted lines for large, medium and small excesses, respectively). Symbols with error bars show observed A-star statistics. At 24 μm, the model predicts too many stars with large excesses at the earliest times, and a monotonic decline in the overall fraction of stars with excesses. There are no new 70 μm data so the right-hand panel is the same as Wyatt et al. (2007b) Fig. 2.

times partly with a formal χ^2 measure for the 24 and 70 μm statistics and the r_{24-70} distribution, but also the success of the model at reproducing trends in the data. In some cases, we can rule out models based purely on a poor fit to the statistics for the older A-stars, in which case our conclusions are independent of the low significance of trends for the younger stars.

4.3 Pre-stirred discs

To illustrate the shortcomings of the pre-stirred model for young stars, the best-fitting parameters from Wyatt et al. (2007b) are compared to the A-star observations in Fig. 6. This figure uses the model of Section 2 with $t_{\rm stir} = 0$ so that discs are pre-stirred. The parameters are: $Q^\star_{\rm D} = 150$ J kg^{-1}, $D_{\rm c} = 60$ km, $e = 0.05$ and a planetesimal belt radius distribution $N(r) \propto r^\gamma$ with $\gamma = -0.8$ and disc width d$r = r_{\rm mid}/2$. We find that $\eta_{\rm mid} = 0.2$ gives the best results (Wyatt et al. specified the disc mass distribution with $M_{\rm mid} = 10\,M_\oplus$). The figure shows that the model still reproduces the 24 and 70 μm A-star statistics for stars 100 Myr and older, but fails to reproduce the trend in large and overall excesses for younger stars at 24 μm. The model shows only a monotonic decline in the overall fraction of stars with excesses in contrast to the observations.

As a metric for comparing models, we quote the χ^2 value at 24 and 70 μm, for the distribution of radii r_{24-70}, and the sum of all three. These are computed as the sum of squared differences between the data and model divided by the Poisson error for all 18 data points at 24 μm (six age bins and three excess bins), 12 points at 70 μm (four age and three excess bins) and five points for the r_{24-70} distribution. In the pre-stirred case shown in Fig. 6, the values are $\chi^2_{24} = 32.4$, $\chi^2_{70} = 5.2$ and $\chi^2_{\rm r} = 17.0$, for a total of $\chi^2_{\rm tot} = 54.6$. Though these numbers give no indication of why a particular model succeeds or fails, or whether it reproduces the desired trends, they formally show how well the statistics are reproduced and provide a benchmark for measuring the success of different self-stirring models.

4.4 Delayed stirring: the simplest case

By taking the peak in large excesses at 10 Myr as an indication of the delay time, we can add the simplest possible model of delayed stirring to our model. Fig. 7 shows a model with almost the same parameters as the pre-stirred model with the addition of a 10 Myr delay (1σ width 0.1 dex) before the onset of stirring for all discs (here $\eta_{\rm mid} = 0.25$). After this delay all discs begin evolving, regardless of radius. This simple modification to the model reproduces the 24 μm excesses better than the pre-stirred model with some change at 70 μm, yielding $\chi^2_{24} = 19.9$, $\chi^2_{70} = 12.5$ and $\chi^2_{\rm r} = 21.9$ for a total

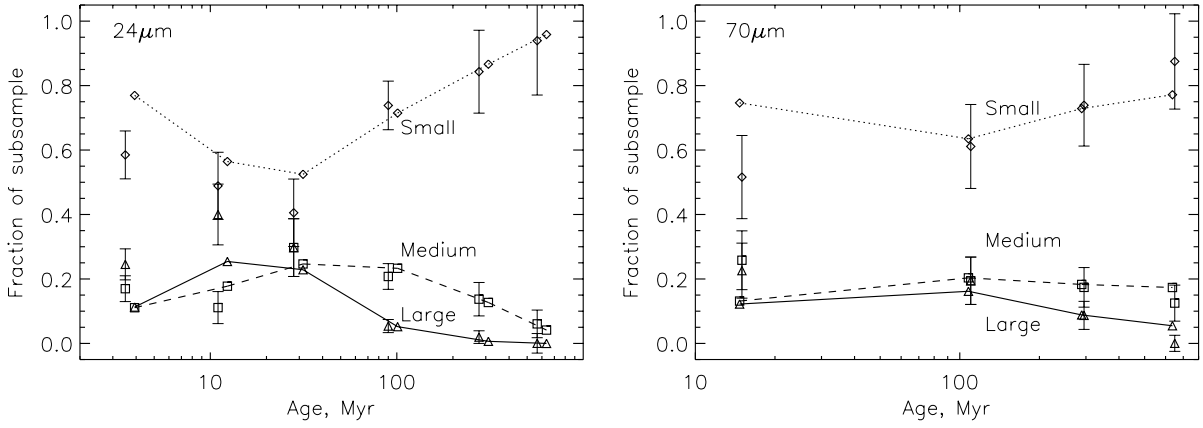

Figure 7. Simple delayed stirring model compared with 24 and 70 μm statistics. Symbols and lines are as in Fig. 6. All discs begin their evolution after ∼10 Myr.

of $\chi^2_{\rm tot} = 54.3$. The three 24 μm excess bins now show the right general trends: the large excesses peak at 10 Myr, the medium excesses show a broad peak over 10–100 Myr and the small excesses reach a minimum around 10–30 Myr. The fraction of small 70 μm excesses at the earliest times increases due to more unstirred discs. An obvious physical motivation for this prescription is unclear, though there are some possibilities that may merit further study.

One possibility might seem to be objects emerging from a protoplanetary disc phase somewhat longer than the 'typical' 6 Myr lifetime (e.g. Haisch, Lada & Lada 2001). However, this explanation is unlikely for two reasons. Primarily, only a small fraction of stars have long lived discs, not the ∼40 per cent suggested by Fig. 4. Further, primordial disc lifetimes around A-stars are consistently shorter than for less massive stars (Kennedy & Kenyon 2009). Therefore, the delay between primordial disc dispersal and the creation of large 24 μm excesses is too long for a plausible direct link.

A possible delay mechanism is scattering of protoplanets and embryos to unstirred locations in the outer disc, where they stir smaller objects to collision velocities. In this scenario, the same fraction as in the 10 Myr peak, ∼40 per cent, of stars must harbour planets that undergo scattering events. This figure is higher than the fractions of intermediate mass stars both known (9 per cent for 1.3–1.9 $M_\odot$; Johnson et al. 2007) and predicted (∼20 per cent for 2–3 $M_\odot$; Kennedy & Kenyon 2008) to have gas giants. However, stellar systems may contain many more undetectable lower mass and/or more distant planets so the fraction of stars with planetary systems is probably not a major problem for this scenario.

The main issues with a scattering scenario are timing and depletion. For all scattering events to occur at around 10 Myr seems to produce a fine tuning problem, when simulations of scattering around solar-type stars show that instabilities can happen at a wide range of epochs. For example, in the case of the 'Nice' model for the late heavy bombardment (LHB) in the Solar system, Gomes et al. (2005) show that the LHB epoch varies strongly with the primordial Kuiper Belt's inner edge location. In addition, this type of simulation is very sensitive to the initial conditions and it is unlikely that all systems undergo instability at any particular time.

The way that planetesimal belts are depleted during scattering events also presents a problem. Based on an analysis of the Nice model, Booth et al. (2009) show that the signature of an LHB like event is a drop in 24 and 70 μm excess ratios of around four orders of magnitude with a brief (∼15 Myr) peak in 24 μm excess, meaning that excess fractions should drop, not peak when LHBs occur. Therefore, planet–planet scattering is an unlikely source of the trends seen in the 24 μm A-star statistics.

Another delay mechanism arises if planetesimals are initially large ('born big', Morbidelli et al. 2009). The lack of an initial population of small grains means that observable dust is not generated until the large planetesimals collide and begin to decay, thus causing a rise and subsequent fall in the small dust population. This delay could plausibly be 10–30 Myr depending on the planetesimal properties and locations.

4.5 Self-stirring

We now turn to the self-stirring model. As discussed in Section 3.1, $D_{\rm c}$ is of the order of 10 km. The eccentricity when 1000 km objects form in the Kenyon & Bromley models is roughly constant with radius, and around $e = 0.01$. We therefore use these numbers as a order of magnitude guide and attempt to reproduce the A-star statistics with similar values. The remaining model parameters are $Q^\star_{\rm D}$, $\eta_{\rm mid}$ and the disc radii. For self-stirring, $x_{\rm delay}$ has little impact on the results (see Section 3.2). Of particular importance is the inner hole specified by $r_{\rm in}$ (or the minimum $r_{\rm mid}$ for narrow belts), needed to ensure a peak in the overall fraction of stars with discs.

We consider two types of discs in our population models. These discs are motivated by observations that show debris discs are commonly narrow belts, in contrast to the structure of protoplanetary discs that extend from several stellar radii to hundreds of astronomical units. Though resolved observations may not discern between a truly narrow belt and an annulus of bright emission in an extended disc, Fig. 3 shows that the excesses for these discs evolve quite differently. Comparing population models to the A-star statistics may therefore suggest which kind of disc is more common. Because protoplanetary discs are the precursors of debris discs, knowing whether they have the same spatial extent will yield information about likely mechanisms and locations for planetesimal and planet formation.

4.5.1 Narrow belts

Fig. 8 shows the model that best reproduces the A-star trends for narrow belts. Belt radii are taken from a distribution with $r_{\rm mid} = 15$–120 au and $\gamma = -0.8$. Belts have width $\mathrm{d}r = r_{\rm mid}/2$, $Q^\star_{\rm D} = 45$ J kg^{-1} and $\eta_{\rm mid} = 0.15$. We set $D_{\rm c} = 10$ km and $e = 0.025$, which are similar to the values expected from the Kenyon & Bromley (2008) models. The fit has improved significance over the pre-stirred and simple delay models with $\chi^2_{24} = 22.4$, $\chi^2_{70} = 15.0$, $\chi^2_{\rm r} = 2.1$ and $\chi^2_{\rm tot} = 39.5$. Initially, we expected that the 10–30 Myr delay for the rise in excesses would lead directly to an inner disc radius using equation (9) for $t_{\rm stir}$. Therefore, with $\eta \sim 0.15$, we expect $r_{\rm mid,min} \sim 30$ au for stirring to occur around 10 Myr (equation 9). However, setting $r_{\rm mid,min}$ to values larger than ≈15 au means that fewer discs are concentrated at small radii, and the distribution of inferred radii and the 70 μm excesses become inconsistent with the observations (see Section 4.6). Because we cannot simultaneously reproduce the statistics and have a peak in large excesses at 10 Myr, it is actually the 70 μm excesses and r_{24-70} distribution that sets $r_{\rm mid,min}$. The timing of the medium excess peak is partly set by $Q^\star_{\rm D}$ because many of these discs decay from younger large excess discs. The relative fractions in the excess bins are set by the distribution of surface densities.

Though a reasonable fit to the 24 and 70 μm statistics and overall distribution of radii is possible, there is some difference in the distribution of radii with time (Fig. 8, lower right-hand panel). At 100 Myr, the lower envelope of model disc radii starts to increase from 15 to ∼60 au by 800 Myr. This change is caused by the decay of smaller discs below detectable levels. Seven discs lie well away from the region populated by the model. The most discrepant discs are the same six noted by Wyatt et al. (2007b) when compared to the pre-stirred population model. All discs with radii less than 10 au have $f/f_{\rm max} > 20$ and may therefore be transient (HDs 38678, 115892, 3003 and 172555). The potential influence of PR drag was offered as an explanation for the remaining two, HD 2262 and HD 106591, which we maintain here and also apply to HD 97633.

As discussed in Section 3.2, we expect self-stirred debris discs to have stirring times similar to their collisional times (i.e. $\mathcal{R} \sim 10^6$). For the narrow belt model, we find that the $\mathcal{R}$ distribution peaks around 2×10^6 with nearly all discs within ±1 dex.

In summary, we find a reasonable fit to the A-star statistics for self-stirred planetesimal belts with physically plausible parameters.

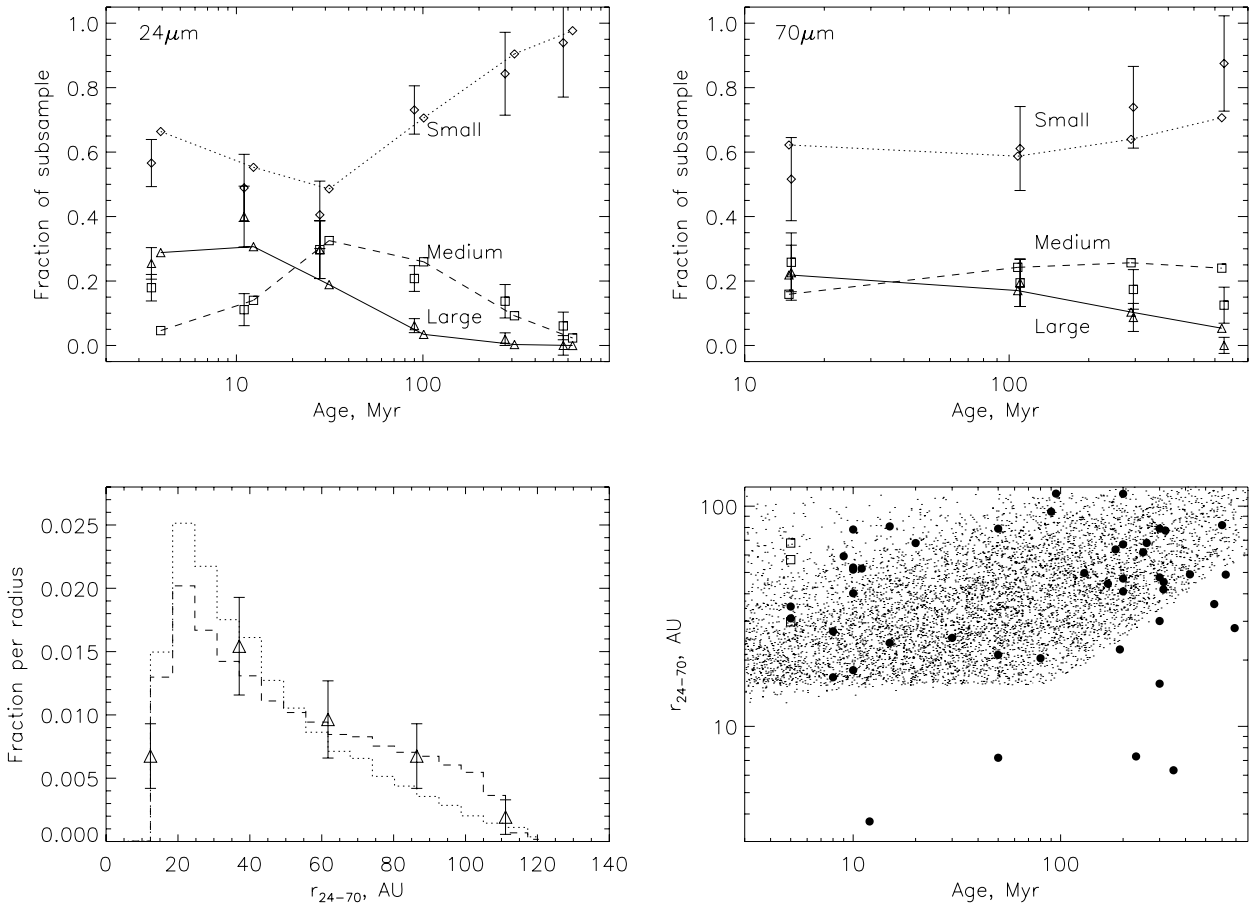

Figure 8. The best fit of the model population to 24 and 70 μm statistics with narrow belts. Top left- and right-hand panels: binned 24 and 70 μm evolution; lower left-hand panel: overall (dashed line) and detectable (dotted line) model r_{24-70} (omitting the four possibly transient sources noted in the text), and lower right-hand panel: r_{24-70} versus t compared to the 46 star subsample (open squares show three additional sources detected by Carpenter et al. 2009, HIP 76310, HIP 77911 and HIP 80088).

The model does not show a strong peak in large 24 μm excesses at 10 Myr because the disc masses and minimum belt radii required mean that many of the smallest discs are stirred at their inner edges before they are observed. However, the model does reproduce all A-star statistics and trends at both 24 and 70 μm.

4.5.2 Extended discs

We consider three possible populations of extended discs, loosely motivated by potential processes that may shape protoplanetary and debris discs: (i) discs with some fixed inner hole size of a few tens of astronomical units that extend to some variable outer radius, perhaps due to their natural size or truncation by stellar encounters or companions, (ii) discs with a fixed outer radius and a variable inner hole size, perhaps cleared by planets that form at various locations and (iii) discs with fixed inner and outer radii, similar in structure to young protoplanetary discs. We do not consider discs with both variable $r_{\rm in}$ and $r_{\rm out}$ because these are effectively a mix of belts and extended discs and provide little useful information about which type of disc is more likely. We again use $D_{\rm c} = 10$ km and $e = 0.01$ as a starting point. When it is fixed, we set $r_{\rm out} = 150$ au. The variable inner or outer radii are chosen from a power-law distribution between the maximum and minimum with power-law index γ.

For the most extended discs, those with fixed $r_{\rm in}$ and $r_{\rm out}$, a reasonable fit to the 24 μm statistics can be found with $r_{\rm in}$ around 40 au ($\chi^2_{24} \sim 35$), but the 70 μm statistics and radius distributions are significantly different ($\chi^2_{70} \sim 190$ and $\chi^2_{\rm r} = 50$). Similarly, for variable $r_{\rm in}$ with $\gamma = -0.8$ and fixed $r_{\rm out}$, good fits to the 24 μm statistics ($\chi^2_{24} \approx 30$) and radius distribution ($\chi^2_{\rm r} \approx 5$) can be achieved, but at the cost of a poor fit to the 70 μm statistics ($\chi^2_{70} \sim 120$). The high χ^2_{70} in both cases is due to ∼40–50 per cent of the model population having medium 70 μm excesses at late (>300 Myr) times.

This high fraction can be understood by looking at how extended discs evolve, shown in Figs 1 and 3. While the 24 μm excess declines as stirring moves further out in the disc, 70 μm excesses for extended discs only show small decreases while the disc is still being stirred. The $\eta = 1/3$ disc in Fig. 1 (middle solid curves) has a 24 μm excess >2 between 7–100 Myr, and would thus contribute to the large 24 μm excess peak in the population model. The 70 μm excess for the same disc rises above the medium excess ratio of 5 at 6 Myr, and remains higher until after 1 Gyr. Even when stirring reaches the outer disc edge, the strong radial dependence on the collisional time means that at ∼100 au the excess only decreases slowly. Therefore, extended discs with fixed $r_{\rm out}$ that have large 24 μm excesses at early times have medium (or large) 70 μm excesses for long periods of time. This evolution means that the A-star statistics rule out self-stirred extended discs with fixed outer radii that evolve like our model. This conclusion is independent of the significance of the 24 μm trends for the younger A-stars.

Though fixed $r_{\rm out}$ leads to problems with the 70 μm excesses at late times, this issue can be addressed by allowing $r_{\rm out}$ to vary. With fixed $r_{\rm in} = 15$ au and the distribution of $r_{\rm out}$ set with $\gamma = -0.8$, the 70 μm statistics can be reasonably reproduced ($\chi^2_{70} \sim 6$). However, this radius distribution has trouble reproducing the 24 μm statistics ($\chi^2_{24} \approx 100$) and the r_{24-70} distribution for the 46 star subsample, predicting too many discs with small radii ($\chi^2_{\rm r} \approx 13$). Attempts to remedy this problem by increasing the number of wider discs (increasing the power-law index γ) results in essentially fixing $r_{\rm out}$, which leads to the previous problem of too many medium excess discs at 70 μm at late times. Thus, extended discs with fixed $r_{\rm in}$ also have trouble reproducing the A-star statistics.

The conclusion that extended discs cannot reproduce the A-star statistics may depend on the particular simplifying assumptions needed to make an analytic population model. A possible key difference is illustrated by Fig. 1: the Kenyon & Bromley (2008) models decay at 70 μm more rapidly than ours and the excesses are ∼2–5 times lower after 100 Myr, probably due to continued accretion and stirring (see Section 3.1).

Whether continued accretion and stirring will lower the predicted 70 μm excesses for extended discs at late times without making the radius distribution significantly steeper (i.e. more discs at large r being undetectable) is not clear, but the comparison in Section 5.2.1 of Kenyon & Bromley (2009) gives some indication. Their model predictions of 70 μm excess fractions for discs with fixed $r_{\rm in}$ and $r_{\rm out}$ are several times higher than the Su et al. (2006) observations at the latest times, as we found in Section 4.5.2. Therefore, it appears that extended disc models that include continued accretion and stirring still evolve too slowly at 70 μm, providing further evidence for the belt-like nature of debris discs.

4.5.3 Summary

Our population model suggests that debris discs are more likely to be narrow belts than extended discs. The formal χ^2 for narrow belts is an improvement over the pre-stirred model, and reproduces all A-star statistics, including the rise and fall in 24 μm excesses. The inability of extended discs to reproduce the statistics is due to how they evolve. Discs with fixed $r_{\rm in}$ predict too many discs at small radii and discs with fixed $r_{\rm out}$ predict too many 70 μm medium excess discs at late times.

The reason belts work well appears to be because they restrict the evolution of excesses. The power-law distribution of $r_{\rm mid}$ means that most discs are at relatively small r, and the evolution is truncated when stirring reaches the outer edge (see Fig. 3). The r_{24-70} distribution is therefore a closer reflection of the initial power-law distribution, rather than being set by self-stirred disc evolution as for extended discs.

4.6 Constraints on the best-fitting model

With the self-stirring model we have somewhat more power to constrain parameters than the Wyatt et al. (2007b) pre-stirred model. This ability arises because we have estimates of $D_{\rm c}$ and e based on the Kenyon & Bromley (2008) results. The remaining parameters left to fit the statistics are $Q_{\rm D}^\star$, $\eta_{\rm mid}$ and the disc radii parameters $r_{\rm mid,min}$ and γ.

For the belt model surface density, we find $\eta_{\rm mid} = 0.15$ gives the best fit. Because we find that debris discs tend to be belts, our use of a surface density law has only a minor impact on our model. There is a factor of 5 difference in surface density from inner to outer disc edges, much smaller than the range of η we consider. Consequently, the model does not strongly constrain the initial surface density power-law index δ. For our best-fitting model we use $\delta = 1.5$, but find that populations with $\delta = 1$ produce similar results.

We find $Q_{\rm D}^\star = 45$ J kg^{-1} gives the best fit to the peak in medium 24 μm excesses, similar to that used for the comparison in Section 3.1. This value is best considered an effective value for the evolution, since a range of $Q_{\rm D}^\star$ are expected for different size planetesimals and at different radii. Our $Q_{\rm D}^\star$ is reasonable for weak rock and ice for $D \sim 10$ km for the ∼100–1000 m s^{-1} range of collision velocities (Leinhardt & Stewart 2009). The value of 45 J kg^{-1} is a third of that found for the best-fitting model in Wyatt et al. (2007b), but as in that paper $Q_{\rm D}^\star$ and e are degenerate. Thus, our results do not change if ${Q_{\rm D}^\star}^{5/6} e^{-5/3} \approx 11\,100$. Löhne et al. (2008) show that the assumption of a single planetesimal strength is within an order of magnitude of a more complex model that includes a size-dependent planetesimal strength (their fig. 11), with the largest differences occurring at late times $\gtrsim$1 Gyr.

Constraining the range of disc radii within the narrow belt model is also possible to some degree. The model has trouble producing a stronger peak in large excesses at 10 Myr while retaining a reasonable fit to the statistics. The model shows a slightly stronger peak in large excesses at 24 μm when the minimum $r_{\rm mid}$ is increased to 20 au, but the fit to the 70 μm excess fractions becomes worse because the relative fraction of wider discs increases (for fixed γ). Therefore, at late times there are more discs with medium 70 μm excesses, essentially the same problem faced for extended discs with fixed $r_{\rm out}$. We find it difficult to fit the A-star statistics with $r_{\rm mid,min} \gtrsim 20$ au (where $\chi^2_{24} = 32.5$, $\chi^2_{70} = 24.8$, $\chi^2_{\rm r} = 5.2$ and total $\chi^2_{\rm tot} = 62.5$).

On the other hand, decreasing the inner hole size actually betters the formal significance of the model fit to the A-stars. With $r_{\rm mid} = 3$–120 au and $\eta = 0.45$, we find $\chi^2_{24} = 14.0$, $\chi^2_{70} = 6.6$, $\chi^2_{\rm r} = 10.6$ and $\chi^2_{\rm tot} = 31.2$. This model shows a monotonic decline in excesses as for the pre-stirred model. However, in contrast to our favoured belt model, this model predicts a population of discs younger than 100 Myr with r_{24-70} less than 15 au. This region is empty in the lower right-hand panel of Fig. 8 (though we ignore discs we deem to be transient). Thus, while the typical minimum belt radius could lie between 3–15 au, we favour the model with minimum belt radii ≈15 au.

The power-law distribution of disc radii is fairly well constrained to $\gamma \approx -0.8$. This constraint arises due to the belt-like nature of discs, which means that the model γ must be similar to the observed distribution.

The chosen age distribution has a small effect on the large excess peak at 10 Myr. If we set the minimum age to 1 Myr (instead of 3 Myr based on σ Ori stars), then the peak becomes slightly stronger. The difference arises because including younger stars results in more unstirred discs (with small excesses) in the youngest age bin. Though this effect is minor, it shows that uncertainty in stellar ages can affect the results of the population model.

5 DISCUSSION

In the previous sections, we have shown how self-stirred debris discs evolve. The model makes predictions, some of which can be compared to photometric observations, such as how disc radii inferred from blackbody models are distributed and evolve.

The most basic prediction of this kind for pre- and self-stirred models is that the radial location of peak emission should increase with time (Fig. 2). However, most surveys have failed to find any

evidence for this trend (e.g. Najita & Williams 2005; Su et al. 2006). Rhee et al. (2007) find an apparent increase in disc radii inferred from *IRAS* colours. Unfortunately, all sources with disc radii greater than 100 au – old stars largely responsible for the trend – have yet to be confirmed with new observations (i.e. with *Spitzer*). This picture is also complicated by the expected increase in the lower envelope of radii at late times as close-in discs drop below detection limits (Fig. 8 lower right-hand panel; Wyatt et al. 2007b). Therefore, our model shows that the expected increase in radii may not be as obvious as predicted by equation (11), and that other predictions of self-stirring could be more useful. For example, another prediction of self-stirring is that discs with large radii for their age should have higher than average disc surface density, because these discs stir to large radii the fastest.

However, it is important that these predicted trends are not just compared with photometric observations, because disc models based solely on SEDs can be degenerate and/or uncertain. Resolved imaging is necessary to confirm or correct SED-derived estimates. Imaging is also needed to test predictions such as the surface density profiles shown in Section 3.2. Below we take a detailed look at a subset of resolved debris discs with the aim of comparing observed disc characteristics with those predicted by models.

Also, we have not addressed an alternative possibility to self-stirring, that discs are stirred by secular perturbations from planets not colocated with the disc (Mustill & Wyatt 2009). In this section, we show that a model with $t_{\rm stir}$ set by planet-stirring can reproduce the A-star statistics and suggest that these planets could cause debris discs to be narrow belts. Because both mechanisms can fit the A-star statistics, high-resolution imaging is the best way to differentiate between self-stirring and planet-stirring.

5.1 Self-stirring versus planet-stirring

The fact that the A-star observations are well reproduced with a self-stirring model shows that this mechanism may be important for debris discs. However, self-stirring is not needed as an explanation for systems such as β Pic where a planet is the likely stirrer. It is therefore important to predict features that allow the stirring mechanism to be identified. In the case of individual systems influenced by planets, these features are well known and stem largely from the same influence that causes planetesimal random velocities to increase and collisions to be destructive. Secular perturbations both warp the disc (e.g. β Pic) and cause it to be offset from the star (e.g. Fomalhaut). These features may be imaged directly, or an offset inferred from peri/apocentre glow (e.g. Wyatt et al. 1999). On shorter time-scales, objects on unstable orbits too close to planets are ejected, which can result in sharp disc edges (e.g. Fomalhaut). The remaining way of identifying whether a planet may be the stirrer is to detect it directly (e.g. Fomalhaut, and perhaps β Pic).

Though these features provide a way of inferring a stirring mechanism (and discovering planets), they can only be applied to individual systems. Distinguishing the dominant stirring mechanism at a population level is more difficult, because planet-stirring introduces yet more parameters to the model. To briefly look at whether a planet-stirred population model can reproduce the A-star statistics, we use the stirring time assuming internal perturbers (Mustill & Wyatt 2009)

$$t_{\rm stir} = 5 \times 10^{-5} \, \frac{\left(1-e_{\rm pl}^2\right)^{3/2}}{e_{\rm pl}} \, \frac{r^{9/2} \sqrt{M_\star}}{M_{\rm pl,Jup} \, r_{\rm pl}^3} \qquad (12)$$

in Myr, where the 'pl' subscripts indicate planet properties and r is the disc location where the stirring time applies.

The increased number of parameters allows more flexibility in reproducing the observed A-star statistics. For example, the A-star statistics can be reproduced as well as in Fig. 8 for narrow belts if we set the stirring time with planet properties: $M_{\rm pl} = 0.5\,M_{\rm Jup}$, $e_{\rm pl} = 0.1$, $r_{\rm pl} = r_{\rm mid}/3$. That is, each belt is assumed to have a $0.5\,M_{\rm Jup}$ planet with eccentricity 0.1 located at one third of its average radius.[8] We assume that planets form early – during the protoplanetary disc phase – so the formation time can be ignored. For comparison with the previous models, this planet stirred model has $\chi^2_{24} = 19.7$, $\chi^2_{70} = 7.3$, $\chi^2_{\rm r} = 4.4$ and $\chi^2_{\rm tot} = 31.3$. This example is unlikely to be the only type of planet distribution that reproduces the observations, and shows that distinguishing between self-stirring and planet-stirring is not yet possible by this method. Future studies of this type can use distributions of known exoplanet properties as input, though these are only complete to $\sim$5 au, and discs may be perturbed by planets at much larger radii (e.g. Fomalhaut).

Some other interesting points can be made if discs are stirred by planets. The decreasing upper envelope of 24 μm excesses for A-stars suggests that the stirrers are not too far interior (or exterior) to the disc, because the strong radial dependence on the stirring time means that discs far from their planets will be unstirred early and then luminous at late times. This conclusion explains the success of the above example, where the planet location scales with the disc radius.

Because the stirring time is set by planet properties and not the disc mass, discs can stir in the fast mode and no longer have a maximum surface density $\tau_{\rm eff,max}$ (see Section 3.2). Neighbouring planetesimal orbits can begin to cross at non-zero eccentricity as they precess, so the collision velocity steps from zero to the forced eccentricity times the Keplerian velocity when the disc is stirred (Mustill & Wyatt 2009). We can also derive a condition similar to (10), but now using equation (12) for the stirring time. For an interior planet-stirred disc to evolve in the slow mode:

$$\mathcal{R}_{\rm pl} \equiv \frac{e_{\rm pl}}{\left(1-e_{\rm pl}^2\right)^{3/2}} \, r_{\rm pl}^3 \, M_{\rm pl,Jup} \, r_{\rm stir}^{-2/3} \, M_\star^{-17/6} \times D_{\rm c} \, {Q_{\rm D}^\star}^{5/6} \, e^{-5/3} \, \eta^{-1} > 2.3 \times 10^5 \, . \qquad (13)$$

This relation is qualitatively different to condition (10), because the planet-stirring time increases more strongly with radius than the decay time (see fig. 6 of Mustill & Wyatt 2009). Thus, discs are more likely to evolve in the fast mode at large radii, because the disc is stirred so late that it would have decayed earlier if it were pre-stirred. Parameters that shorten the planet-stirring time, such as higher $e_{\rm pl}$ or $M_{\rm pl}$, or larger $r_{\rm pl}$ (bringing the planet closer to the disc because this example is for interior planets) make the disc more likely to stir in the slow mode.

In summary, a population model of discs stirred by secular perturbations from planets can reproduce the A-star statistics if the planets are located near the disc. This model is unlikely to be unique, as different distributions of planet properties can probably give similar results. Therefore, it is not possible to distinguish between self-stirring and planet-stirring for debris disc populations by this method yet. The features shown by high-resolution imaging of individual objects, such as warps and offsets, remain the best marker of debris discs influenced by planets. Our planet-stirred example also motivates planetary system architecture as a possible reason for debris discs to be narrow belts.

[8] Setting equations (9) and (12) equal and solving for $r_{\rm pl}$ suggests $r_{\rm pl} \propto \sqrt{r_{\rm mid}}$. However, the stronger scaling may be needed to account for the stirring time being independent of disc mass.

5.2 The origin of narrow belts

Returning to the idea that resolved discs can be roughly split into extended discs and belts (Kalas et al. 2006), our results suggest that debris discs tend to be narrow belts that have minimum radii of ∼15 au. A similar conclusion was reached by Chen et al. (2006), who found that most of their objects' Spitzer IRS spectra were best fit by single temperature blackbodies colder than 130 K (thus also suggesting that discs have inner holes). In contrast, nearly all young stars have evidence for protoplanetary dust and gas discs that extend from very near the star (e.g. Haisch et al. 2001) to hundreds of au (e.g. McCaughrean & O'Dell 1996; Watson et al. 2007). The implication is that not only the primordial disc extent sets where debris discs reside, but other influences such as photoevaporation, disc fragmentation and truncation and clearing by planetary and stellar companions. Within the context of the previous section, planets that stir the disc may also be responsible for clearing it at other locations. As is likely the case with β Pic (Augereau et al. 2001), apparently extended discs may result from the blowout of small grains created in a relatively narrow planetesimal belt.

To produce debris discs that are narrow belts, these mechanisms need to plausibly reproduce two qualitative trends: (i) disc inner and outer radii are positively correlated because we find that they are narrow belts and (ii) most discs have relatively small radii, to reproduce the observed power-law distribution of disc radii.

One possibility is that the belts are locations where planetesimal formation was possible or favoured. For example, one process that both clears dust from inner regions and enhances more distant regions is the influence of photoevaporative disc clearing. Alexander & Armitage (2007) show that after the inner gas disc has cleared, small grains ($\lesssim$10–100 cm) are dragged outwards as the inner edge of the gas disc moves outwards. At some point, the gas disc either becomes too tenuous to keep moving the grains, or the dust density becomes comparable to the gas density. Either way, a concentrated mass of grains is left behind by the gas (though objects larger than ∼1 m are less affected by this process). Formation of Pluto-size objects will be enhanced here, either simply due to the faster growth time, or a more rapid instability (e.g. Youdin & Shu 2002). Another mechanism that may result in an inner hole and planetesimals at a particular location is the direct or rapid formation of planetesimals in the spiral arms of a self-gravitating disc (Rice et al. 2006; Clarke & Lodato 2009). This process necessarily occurs beyond tens of astronomical units where the disc is marginally stable and dust may be concentrated in spiral arms on a time-scale shorter than the orbital period. This process may result in narrow belts, because at $\gtrsim$100 au distances the disc is unstable to fragmentation and may form companions that truncate the disc. However, given that only ∼10 per cent of the Su et al. (2006) sample have known companions, binary truncation seems an unlikely process for setting disc outer radii.

The alternative is that the belts are locations where systems are able to retain planetesimals. For example, one possibility is truncation by exterior stellar companions, or within a cluster environment. However, stellar flybys are unlikely to be what sets disc outer radii because the cross-section for a close encounter suggests that this mechanism should more often result in large discs, rather than small ones.

Planet formation provides a possible explanation of debris disc radii, and is naturally consistent with both self-stirring and planet-stirring models. It is reasonable to think that planetesimals form out to radii some fraction farther than where planets can form. Dynamical clearing by planets can then set disc inner radii, analogous to how Solar system planets dictate the Asteroid and Kuiper belt locations. In this picture, debris disc systems therefore consist of an inner planetary system with some radial extent and a narrow planetesimal belt that extends somewhat further. This picture is essentially that of the planet-stirred example that reproduces the A-star statistics above in Section 5.1.

The range and distribution of disc radii may be linked to the initial protoplanetary disc mass. Higher surface density discs are expected to form more giant planets over a wider range of radii (e.g. Kennedy & Kenyon 2008) and these systems are likely more susceptible to scattering, resulting in more extended dynamical clearing and debris discs with larger inner radii (and provides a simplistic explanation for why the BPMG and TW Hydrae A-star discs with the largest excesses have the largest radii as discussed below). If most protoplanetary discs are relatively low mass (e.g. Andrews & Williams 2005), this scenario would also typically result in debris discs at relatively small radii in agreement with the r_{24-70} from our A-star sample.

The degree to which planets influence debris disc structure probably varies. In some cases, planets may simply dynamically clear inner regions while the rest of the disc is self-stirred, whereas in other cases the disc structure may be entirely set by migration and shepherding, scattering and secular stirring. We now turn to a small sample of resolved A-stars that allow us to study these possibilities for individual systems.

5.3 Comparison with resolved imaging

Resolved debris discs that show structures such as warps and offsets reveal planets that may remain otherwise invisible. In these cases, planet-stirring is probably more important than self-stirring. Therefore, resolved imaging allows estimation of the stirring mechanism in individual cases.

Resolved imaging also allows other comparisons between observations and models to be made, such as with the surface density profiles shown in Fig. 2. Though the distribution of radii in our model is set by comparing model and observed r_{24-70}, this measure tends to underestimate disc radii and cannot account for discs with several dust components, providing further motivation for imaging.

As a sample of resolved debris discs, we use stars in the ∼12 Myr old BPMG (Zuckerman & Song 2004) and the similarly aged ∼8 Myr old TW Hydrae Association. This sample is therefore roughly coeval and about the age of the 24 μm excess peak.

The A-stars in this sample are HR 4796A (HD 109573), β Pic (HD 39060), η Tel (HD 181296), HR 7012 (HD 172555), HR 6070 (HD 146624) and HR 6749/HR 6750 (HD 165189/HD 165190). Of these, HR 6070 and HR 6749/6750 have no excesses at 24 or 70 μm (Rebull et al. 2008). Characteristics of the remaining four are shown in Table 1. The actual radii ($r_{\rm real}$) of HR 4796A and β Pic are several times larger than r_{24-70}, and in reasonable agreement for HR 7012 and the outer dust component of η Tel. The difference in the case of β Pic and HR 4796A is explained by the presence of small grains, which emit inefficiently at long wavelengths, and are thus hotter than a blackbody grain at the same stellocentric distance.

Compared to the entire A-star sample, the 24 μm excesses in this 10 Myr sample are among the largest (see Fig. 4). Comparing the fraction of stars with discs with $R_{24} \geq 5.5$ (i.e. the same or brighter than η Tel), the ∼10 Myr sample has 67 ± 33 per cent (4/6) while the fraction for the remaining stars in the 6–20 Myr age bin in the overall A-star sample is 8 ± 5 per cent (3/38). Whether this relatively high excess fraction is the result of evolution within a low-density association or simply due to a small sample size is unclear.

Table 1. BPMG and TW Hydrae A-stars with discs.

Name	r_{24-70} (au)	$r_{\rm real}$ (au)	$L_{\rm disc}/L_\star$	R_{24}
HR 4796A	27	70	330e-5	97
β Pic	24	70	140e-5	26
HR 7012	4	0.9, 6	50e-5	5.9
η Tel	25	3.9, 24	20e-5	5.5

Note. Inferred disc radii r_{24-70} and $f = L_{\rm disc}/L_\star$ from Wyatt et al. (2007b). Real disc radii $r_{\rm real}$ are derived from imaging and modelling (β Pic and HR 4796A, Schneider et al. 1999, 2009; Augereau et al. 2001; Telesco et al. 2005) or detailed SED modelling (Chen et al. 2006; Smith et al. 2009). The fractional luminosities $R_{24} = F_{24,\rm tot}/F_{24,\star}$ are from Rebull et al. (2008) and Rieke et al. (2005).

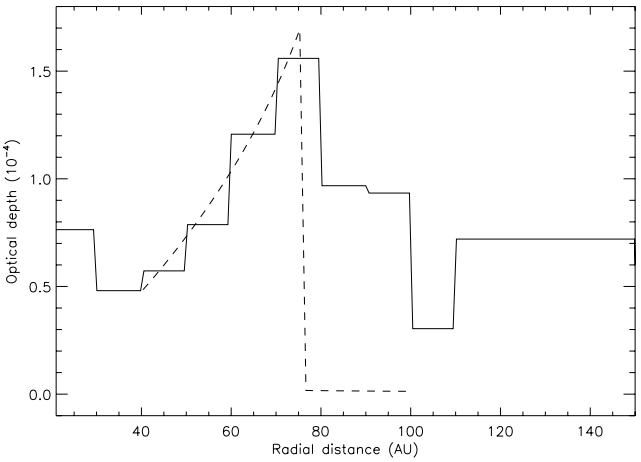

Figure 9. Optical depth in the β Pictoris debris disc derived from mid-IR imaging (Telesco et al. 2005). Overplotted is the $\tau_{\rm eff}$ profile for a secular-stirred planetesimal belt (dashed line) between 40–100 au (see text for details).

Starting with β Pic, this star harbours the second brightest known debris disc, which appears extended in both scattered light and at IR and longer wavelengths (e.g. Smith & Terrile 1984; Chini et al. 1991; Holland et al. 1998; Telesco et al. 2005). The disc appears over a wide range of radii, at least partly due to blowout of small grains created in collisions (Augereau et al. 2001). Modelling of the scattered light and mid-IR emission suggests that the parent disc where these grains originate is centred at around 70–80 au (Augereau et al. 2001; Telesco et al. 2005). In addition, a $\sim$10 $M_{\rm Jup}$ planet at $\sim$10 au has been inferred as the cause of a warp in the disc (Mouillet et al. 1997) that reaches a peak near the same location as the parent belt (Heap et al. 2000). This proposed companion has recently been imaged (Lagrange et al. 2009b), though confirmation with second epoch observations is needed (Lagrange et al. 2009a; Lecavelier Des Etangs & Vidal-Madjar 2009). Finally, Telesco et al. (2005) find an apparent clump of small grains in the south-west wing of the disc at $\sim$50 au.

The solid line in Fig. 9 shows the optical depth profile of β Pic derived from mid-IR imaging of β Pic (north-east wing; Telesco et al. 2005). The optical depth peaks at around 75 au, with a decrease to larger and smaller radii. This profile suggests that the disc has been stirred to 75 au. Comparison with Fig. 2 suggests that the profile is more akin to a fast self-stirred disc because the profile drops immediately interior to 75 au. That is, the collisional time is shorter than the stirring time at $r_{\rm stir}$ so condition (10) is not satisfied. As discussed in Section 3.2, this profile is unlikely to be the result of self-stirring (though can be fit with a self-stirred model).

There are, of course, other possible explanations for the origin of the β Pic optical depth profile. The surface density of small grains interior to 75 au may drop more rapidly due to continued accretion and stirring by Pluto-size objects for example. Alternatively, if we still assume that the profile is due to collisional evolution, planet-stirring is a possible scenario. As noted is Section 5.1, this evolution can produce discs that stir in the fast mode. Indeed, a planet has already been proposed as the cause for a warp in the β Pic disc, and the maximum extent of the warp suggests that stirring due to the planet has reached $\sim$75 au, the location of the peak optical depth.

The dashed line in Fig. 9 shows the optical depth profile of a planet-stirred model with good agreement between 40–80 au. The model has a planet with mass $M_{\rm pl}/{\rm M}_\odot = 16 \times 10^{-3}$ at $a_{\rm pl} = 10$ au with $e_{\rm pl} = 0.1$, and the disc is therefore stirred to $\sim$75 au in 12 Myr (though equation 12 shows that $M_{\rm pl}$, $a_{\rm pl}$ and $e_{\rm pl}$ are degenerate in setting $t_{\rm stir}$). The value $e = 0.025$ is roughly the forced eccentricity set by the planet which in turn sets the collision velocities as $\sim$150 m s^{-1}. For the disc to be depleted interior to 75 au, we need fairly small planetesimals, with $D_{\rm c} = 0.1$ km, $Q_{\rm D}^\star = 40$ J kg^{-1} and $\eta = 0.01$. To match the overall level of optical depth requires decreasing q to 1.8 (from 1.83). The collision velocities may be higher due to increased planetesimal inclinations, expected if the planet is inclined relative to the disc, which is the interpretation of the observed warp (Mouillet et al. 1997; Augereau et al. 2001). In this case, a model with larger planetesimals can reproduce the observed optical depth profile.

To match the optical depth exterior to 80 au requires very large $x_{\rm delay} \sim 0.5$. It is more likely that the emission outside 80 au is due to small grains created in collisions at <80 au being blown out of the system, thus making the disc appear more extended than it really is (Augereau et al. 2001). Because we infer small $D_{\rm c}$, an alternative explanation for the clump of small grains in the south-west wing at about 50 au is needed, because the clump has about as much mass as a 100 km planetesimal (Telesco et al. 2005). Collective phenomena such as resonance trapping (Wyatt 2003) or dust avalanches (Grigorieva, Artymowicz & Thébault 2007) would be required to explain the clump.

The disc around HR 4796A has a similar radius to β Pic. Detailed modelling suggests a $\sim$15 au wide parent belt at 70 au with a wider distribution of smaller blowout grains (Wahhaj et al. 2005). As with β Pic, this disc is unlikely to be self-stirred. The relatively sharp inner disc edge and a brightness asymmetry and possible offset (e.g. Telesco et al. 2000; Wahhaj et al. 2005; Schneider et al. 2009), make HR 4796A reminiscent of the Fomalhaut disc, which is known to harbour an interior planet that may affect the disc (Chiang et al. 2009). If the inner edge of the HR 4796A disc is truncated by a planet, then it is probably stirred by that planet.

The two remaining discs, those around HR 7012 and η Tel, are fainter than the previous two, but still have large excesses relative to the overall A-star sample. HR 7012 has a very small disc, with detailed models of IRS spectra suggesting grain temperatures corresponding to 0.9–6 au (Chen et al. 2006). These models require sub-μm-sized grains, with a composition indicative of dust produced in a recent collision (Chen et al. 2006; Lisse et al. 2009). The mass of grains inferred is of the order of 10^{21} g, the mass contained in a planetesimal a few tens of km in diameter. This disc has an unusually small radius for its age (Wyatt et al. 2007b) and a reasonably high $f/f_{\rm max} \sim 100$, also suggesting that the dust is likely transient and not due to self-stirring. However, this conclusion does not mean that the disc was never self-stirred. To have reached what

may be an analogous stage to the giant-impact period that formed the Solar system's terrestrial planets, objects orbiting HR 7012 almost certainly went through the stages of growth where self-stirring is expected. This late stage of chaotic growth could be considered a second phase of self-stirring, where the stirring this time arises because the surface density of smaller objects is insufficient to damp the largest objects and big objects stir each other.

Finally, η Tel has distinct planetesimal belts at $\sim$4 and 24 au, each contributing about equally to the excess at 24 μm (Chen et al. 2006; Smith et al. 2009). Smith et al. (2009) find that the outer disc can be explained by a self-stirred model. If stirring has reached 24 au, the hotter dust may be the result of a collision as planets continue to grow in inner regions. In contrast to HR 7012, however, there is no evidence for sub-μm grains in the η Tel disc from which it might be inferred that a recent collision is required to explain short lived dust (Chen et al. 2006).

In summary, when confronted with detailed observations, the self-stirring model appears to face competition from the continued growth of planets through stochastic collisions and their dynamical effects in trying to provide explanations of disc structure. The β Pic disc is likely stirred by the proposed planet at $\sim$10 au. The non-azimuthal symmetry of the HR 4796A disc also suggests a planetary influence. The η Tel disc is consistent with a self-stirring model and HR 7012 is probably a transient disc resulting from a recent collision.

6 CONCLUSIONS

Recent observations of young A-stars show evidence for an increase in the level and frequency of 24 μm excesses from $\sim$3 to 10–30 Myr (Hernández et al. 2006; Currie et al. 2008a,b). Excesses then decline on an time-scale of $\sim$150 yr (Rieke et al. 2005). The rise in debris disc emission at early times has been interpreted as evidence for self-stirring, where a collisional cascade begins when Pluto-size objects form and stir planetesimals. Because the time taken to form Plutos increases with radial distance from the central star, Wyatt (2008) noted that the 10–30 Myr delay also implied that A-star discs must have inner holes of the order of 10 au if they are self-stirred. Though there is in fact little evidence that the fraction of stars with 24 μm excesses changes in the first 50 Myr or so (Fig. 4), the overall trend shown by the A-star statistics provides tentative observational evidence of self-stirring. However, a promising alternative to self-stirring should also be considered, that debris discs are instead stirred by secular perturbations from an eccentric planet (Mustill & Wyatt 2009).

In this paper, we use the analytic model described in Section 2 to study the evolution of self-stirred discs. Our model is essentially the steady-state evolution model of Wyatt et al. (2007b), modified to include self-stirring. We first compare our model to the detailed Kenyon & Bromley (2008) results, using an empirical delay for self-stirring to ensure we reproduce their excess trends over a range of disc surface densities and stellar masses (Section 3). The only difference in evolution is after the peak excess, with the Kenyon & Bromley models decaying more rapidly at 70 μm, probably due to continued accretion.

We illustrate the implications of collisional evolution for resolved discs (Section 3.2). Because discs process their mass from the inside out, the surface density profile of any collisionally evolved disc region increases as $r^{7/3}$ and discs appear to increase in radius over time (pre- and planet-stirred discs show the same behaviour). The primordial surface density profile remains where the disc has not been stirred (and protoplanetary growth is ongoing).

Discs with delayed stirring can evolve in two different ways. If the collisional time is short compared to the stirring time (i.e. has more mass than it would if it were pre-stirred), then the disc rapidly loses mass as it reverts to its equilibrium state. This evolution results in a bright narrow ring of emission where stirring is occurring (Fig. 2). While we suggest that this evolution is unlikely for self-stirred discs, it can occur for planet-stirred discs. Discs that stir before the collisional time evolve in the same way as pre-stirred discs, with the difference that there is less emission in exterior regions where the collisional cascade has not started. This is the typical evolution we expect for self-stirred discs.

In Section 4, we turn to the observations and show why the pre-stirred debris disc model fails to produce the trends in the A-star statistics; with no mechanism to delay the onset of stirring, 24 μm excesses in the model are highest at the earliest times. The overall fraction of stars with discs declines monotonically with time in contrast with the observations, which peak around 30 Myr. Using the same power-law planetesimal belt radius distribution as Wyatt et al. (2007b), and planetesimal sizes and eccentricities consistent with the Kenyon & Bromley (2008) models, we show that the A-star trends and statistics can be reasonably reproduced by a self-stirring model with $Q_{\rm D}^{\star} = 45$ J kg^{-1} and the average disc mass 0.15 times an MMSN disc. Discs are 'narrow belts' with width d$r = r_{\rm mid}/2$. The smallest planetesimal belt has $r_{\rm mid} = 15$ au and the largest 120 au.

We have less success fitting the A-star observations with extended discs – discs with fixed inner and/or outer radii. Although the 24 μm emission can be reasonably reproduced with discs with fixed $\sim$150 au outer radii and fixed or variable inner radii, these models result in too many 70 μm excess discs at late times. This problem arises because extended discs evolve at near constant 70 μm fractional luminosity until their outer edges are stirred (Figs 1 and 3). Discs with fixed inner radii of $\sim$15 au and variable outer radii also fail to fit the observed statistics, because the models overpredict the number of discs with small radii. Thus, our conclusion that debris discs are narrow belts and not extended is independent of the A-star trends for ages $\lesssim$50 Myr.

Progress can be made in several directions to further understand the effects of self-stirring on model populations. Our model only removes dust from the small end of the size distribution, whereas the Kenyon & Bromley (2008) models show that mass is also lost as Pluto-size objects continue to accrete fragments, and that mass loss is accelerated as the largest objects continue to grow. A model including continued accretion and stirring will lower 70 μm excesses for the oldest discs, perhaps allowing extended discs to reproduce the A-star statistics. However, the Kenyon & Bromley (2009) model comparison with A-star data suggests there will still be difficulties, with extended disc models that include continued accretion and stirring also evolving too slowly at 70 μm.

Planets probably stir and set the structure of some discs. In Section 5.1, we show the A-star statistics can be fit with a population of narrow belts stirred by secular perturbations from an eccentric planet. The planet-stirred model produces essentially the same results as the self-stirred one, with the key to reproducing the A-star observations apparently being the planet location. If planets are located too far from the disc then stirring occurs too late and the characteristic $\sim$150 Myr time-scale decay of 24 μm excesses does not occur. Thus, the successful model has 0.5 $M_{\rm Jup}$ planets with $e = 0.1$ that are located at one third the disc radius.

Therefore, population models cannot yet distinguish whether self-stirring or planet-stirring is more important. Population models are also unlikely to rule out one stirring mechanism due to the

many model parameters. The poor statistics for A-stars younger than ∼50 Myr also hinder progress. The fact that the rise in 24 μm excesses for young A-stars has marginal statistical significance is unlikely to change in the near future, as most nearby regions have been studied with *Spitzer* and a significant increase in numbers awaits the launch of the James Webb Space Telescope.

In Section 5.2, we consider the origin of narrow planetesimal belts, and suggest that planet formation provides a natural explanation, if planetesimals form to radii somewhat larger than planets. The debris disc inner holes are then regions cleared by planets, and the outer extent set by where planetesimals can form. Depending on planetary system architecture, these planets may also stir the disc as suggested by our planet-stirred example in Section 5.1.

In Section 5.3, we look more closely at the sample of ∼10 Myr old resolved discs around A-stars from the BPMG and the TW Hydrae Association, and find that only η Tel allows a reasonable explanation with a self-stirring model. The discs around β Pic and HR 4796A seem more likely to be affected by planets. It is possible that the β Pic debris disc is stirred through secular perturbations from the planet proposed to orbit at ∼10 au. The disc around HR 7012 appears transient, though probably went through a phase of self-stirring when it was younger. These observations suggest that the degree to which debris discs are influenced by planets varies, and that the answer to the question of debris disc stirring lies with high-resolution imaging.

ACKNOWLEDGMENTS

It is a pleasure to thank Ken Rice for helpful discussions, Scott Kenyon for discussions and kindly sharing output from his self-stirring models and Alexander Krivov for a thorough review that improved the content and presentation of this contribution. This study was completed during the Isaac Newton Institute's Dynamics of Disks and Planets programme in Cambridge, UK.

REFERENCES

Alexander R. D., Armitage P. J., 2007, MNRAS, 375, 500
Andrews S. M., Williams J. P., 2005, ApJ, 631, 1134
Andrews S. M., Williams J. P., 2007, ApJ, 671, 1800
Augereau J. C., Nelson R. P., Lagrange A. M., Papaloizou J. C. B., Mouillet D., 2001, A&A, 370, 447
Blum J., Wurm G., 2008, ARA&A, 46, 21
Booth M., Wyatt M. C., Morbidelli A., Moro-Martín A., Levison H. F., 2009, MNRAS, 399, 385
Burns J. A., Lamy P. L., Soter S., 1979, Icarus, 40, 1
Carpenter J. M., Mamajek E. E., Hillenbrand L. A., Meyer M. R., 2009, ApJ, 705, 1646
Chen C. H. et al., 2006, ApJS, 166, 351
Chiang E., Kite E., Kalas P., Graham J. R., Clampin M., 2009, ApJ, 693, 734
Chini R., Kruegel E., Kreysa E., Shustov B., Tutukov A., 1991, A&A, 252, 220
Clarke C. J., Lodato G., 2009, MNRAS, 398, L6
Currie T., Kenyon S. J., Balog Z., Rieke G., Bragg A., Bromley B., 2008a, ApJ, 672, 558
Currie T., Plavchan P., Kenyon S. J., 2008b, ApJ, 688, 597
Dermott S. F., Grogan K., Durda D. D., Jayaraman S., Kehoe T. J. J., Kortenkamp S. J., Wyatt M. C., 2001, in Grun E., Gustafson B. A. S., Dermott S. F., Fechtig H., eds, Interplanetary Dust. Springer-Verlag, Berlin, p. 569
Dohnanyi J. S., 1969, J. Geophys. Res., 74, 2531
Dominik C., Decin G., 2003, ApJ, 598, 626
Gomes R., Levison H. F., Tsiganis K., Morbidelli A., 2005, Nat, 435, 466
Grigorieva A., Artymowicz P., Thébault P., 2007, A&A, 461, 537
Haisch Jr K. E., Lada E. A., Lada C. J., 2001, ApJ, 553, L153
Heap S. R., Lindler D. J., Lanz T. M., Cornett R. H., Hubeny I., Maran S. P., Woodgate B., 2000, ApJ, 539, 435
Hernández J., Briceño C., Calvet N., Hartmann L., Muzerolle J., Quintero A., 2006, ApJ, 652, 472
Hernández J. et al., 2007, ApJ, 662, 1067
Hernández J., Hartmann L., Calvet N., Jeffries R. D., Gutermuth R., Muzerolle J., Stauffer J., 2008, ApJ, 686, 1195
Hernández J., Calvet N., Hartmann L., Muzerolle J., Gutermuth R., Stauffer J., 2009, ApJ, 707, 705
Holland W. S. et al., 1998, Nat, 392, 788
Johnson J. A., Butler R. P., Marcy G. W., Fischer D. A., Vogt S. S., Wright J. T., Peek K. M. G., 2007, ApJ, 670, 833
Kalas P., Graham J. R., Clampin M. C., Fitzgerald M. P., 2006, ApJ, 637, L57
Kalas P. et al., 2008, Sci, 322, 1345
Kennedy G. M., Kenyon S. J., 2008, ApJ, 673, 502
Kennedy G. M., Kenyon S. J., 2009, ApJ, 695, 1210
Kenyon S. J., Bromley B. C., 2004, AJ, 127, 513
Kenyon S. J., Bromley B. C., 2008, ApJS, 179, 451
Kenyon S. J., Bromley B. C., 2009, preprint (arXiv:0911.4129)
Kharchenko N. V., 2001, Kinematika i Fizika Nebesnykh Tel, 17, 409
Lagrange A. et al., 2009a, A&A, 506, 927
Lagrange A. et al., 2009b, A&A, 493, L21
Lecavelier Des Etangs A., Vidal-Madjar A., 2009, A&A, 497, 557
Leinhardt Z. M., Stewart S. T., 2009, Icarus, 199, 542
Lissauer J. J., 1987, Icarus, 69, 249
Lisse C. M., Chen C. H., Wyatt M. C., Morlok A., Song I., Bryden G., Sheehan P., 2009, ApJ, 701, 2019
Löhne T., Krivov A. V., Rodmann J., 2008, ApJ, 673, 1123
McCaughrean M. J., O'Dell C. R., 1996, AJ, 111, 1977
Morbidelli A., Bottke W. F., Nesvorný D., Levison H. F., 2009, Icarus, 204, 558
Moro-Martín A., Malhotra R., 2003, AJ, 125, 2255
Mouillet D., Larwood J. D., Papaloizou J. C. B., Lagrange A. M., 1997, MNRAS, 292, 896
Mustill A. J., Wyatt M. C., 2009, MNRAS, 399, 1403
Najita J., Williams J. P., 2005, ApJ, 635, 625
Natta A., Grinin V., Mannings V., 2000, Protostars and Planets IV. Univ. Arizona Press, Tucson, p. 559
Quillen A. C., 2006, MNRAS, 372, L14
Quillen A. C., Morbidelli A., Moore A., 2007, MNRAS, 380, 1642
Rebull L. M. et al., 2008, ApJ, 681, 1484
Rhee J. H., Song I., Zuckerman B., McElwain M., 2007, ApJ, 660, 1556
Rice W. K. M., Lodato G., Pringle J. E., Armitage P. J., Bonnell I. A., 2006, MNRAS, 372, L9
Rieke G. H. et al., 2005, ApJ, 620, 1010
Schmidt-Kaler T., 1982, in Schaifers K., Voigt H. H., eds, Landolt-Bornstein: Numerical Data and Functional Relationships in Science and Technology, Group VI, Vol. 2. Springer-Verlag, Berlin
Schneider G. et al., 1999, ApJ, 513, L127
Schneider G., Weinberger A. J., Becklin E. E., Debes J. H., Smith B. A., 2009, AJ, 137, 53
Siegler N., Muzerolle J., Young E. T., Rieke G. H., Mamajek E. E., Trilling D. E., Gorlova N., Su K. Y. L., 2007, ApJ, 654, 580
Smith B. A., Terrile R. J., 1984, Sci, 226, 1421
Smith R., Churcher L. J., Wyatt M. C., Moerchen M. M., Telesco C. M., 2009, A&A, 493, 299
Su K. Y. L. et al., 2006, ApJ, 653, 675
Telesco C. M. et al., 2000, ApJ, 530, 329
Telesco C. M. et al., 2005, Nat, 433, 133
Wahhaj Z., Koerner D. W., Backman D. E., Werner M. W., Serabyn E., Ressler M. E., Lis D. C., 2005, ApJ, 618, 385
Watson A. M., Stapelfeldt K. R., Wood K., Ménard F., 2007, in Reipurth B., Jewitt D., Keil K., eds, Protostars and Planets V. Univ. Arizona Press, Tucson, p. 523

Weidenschilling S. J., 1977, Ap&SS, 51, 153
Wyatt M. C., 2003, ApJ, 598, 1321
Wyatt M. C., 2005, A&A, 433, 1007
Wyatt M. C., 2008, ARA&A, 46, 339
Wyatt M. C., Dent W. R. F., 2002, MNRAS, 334, 589
Wyatt M. C., Dermott S. F., Telesco C. M., Fisher R. S., Grogan K., Holmes E. K., Piña R. K., 1999, ApJ, 527, 918
Wyatt M. C., Smith R., Greaves J. S., Beichman C. A., Bryden G., Lisse C. M., 2007a, ApJ, 658, 569
Wyatt M. C., Smith R., Su K. Y. L., Rieke G. H., Greaves J. S., Beichman C. A., Bryden G., 2007b, ApJ, 663, 365
Yi S., Demarque P., Kim Y., Lee Y., Ree C. H., Lejeune T., Barnes S., 2001, ApJS, 136, 417
Youdin A. N., Shu F. H., 2002, ApJ, 580, 494
Zuckerman B., Song I., 2004, ARA&A, 42, 685

This paper has been typeset from a TEX/LATEX file prepared by the author.